Random First Order Theory concepts in Biology and Condensed Matter physics

T.R.Kirkpatrick*

Institute for Physical Science and Technology, and Department of Physics, University of Maryland, College Park, Maryland 20742, USA

D.Thirumalai†

Institute for Physical Science and Technology, and Department of Chemistry, University of Maryland, College, Park, Maryland 0742, USA

(Dated: December 17, 2014)

The routine transformation of a liquid, as it is cooled rapidly, resulting in glass formation, is remarkably complex. A theoretical explanation of the dynamics associated with this process has remained one of the major unsolved problems in condensed matter physics. The Random First Order Transition (RFOT) theory, which was proposed over twenty five years ago, provides a theoretical basis for explaining much of the phenomena associated with glass forming materials. It links or relates multiple metastable states, slow or glassy dynamics, dynamic heterogeneity, and both a dynamical and an ideal glass transition. Remarkably, the major concepts in the RFOT theory can also be profitably used to understand many spectacular phenomena in biology and condensed matter physics, as we illustrate here. The presence of a large number of metastable states and the dynamics in such complex landscapes in biological systems from molecular to cellular scale and beyond leads to behavior, which is amenable to descriptions based on the RFOT theory. Somewhat surprisingly even intratumor heterogeneity arising from variations in cancer metastasis in different cells is hauntingly similar to glassy systems. There are also deep connections between glass physics and electronically disordered systems undergoing a metal-insulator transition, aging effects in which quantum effects play a role, and the physics of super glasses (a phase that is simultaneously a super fluid and a frozen amorphous structure). We argue that the common aspect in all these diverse phenomena is that multiple symmetry unrelated states governing both the equilibrium and dynamical behavior - a lynchpin in the RFOT theory - controls the behavior observed in these unrelated systems.

PACS numbers:

arXiv:1412.5017v1 [cond-mat.dis-nn] 15 Dec 2014

Contents

I. Introduction 2
- A. General remarks on glassy systems 2
- B. Configurational Entropy and the Kauzmann Paradox 2
- C. On the origins of the RFOT 3
- D. Assessment of the RFOT 4

II. Basic notions of the RFOT for the structural glass transition 5
- A. Two transitions 5
- B. The dynamical transition 6
  - 1. Theoretical description 6
  - 2. Experimental evidence for the dynamical transition 7
- C. Dynamics and random field effects below the dynamical transition 8
- D. Entropy crisis and divergent activated transport near the ideal glass transition 8

III. Dynamic heterogeneity, law of large numbers, rare regions, and activated scaling in glassy systems 9
- A. Dynamic heterogeneity 9
- B. Dynamic heterogeneity and violation of law of large numbers 10
- C. Rare region dynamics near the glass transitions 11
- D. Activated scaling near the glass transition 11

IV. Understanding biological problems from the perspective of glass physics 12
- A. Countable number of structural states in the sequence space of proteins 12
- B. Kinetic accessibility and folding rate dependence of proteins and RNA on N 13
- C. Persistent heterogeneity 14
- D. Cellular dynamics 16

V. Glass transition concepts and the RFOT in condensed matter physics 16
- A. Aging in quantum glassy systems 16
- B. Disordered and interacting electrons: Connections with random field problems and the glass transition problem 17
- C. The metal-insulator transition and many-body localization 18
- D. Super glasses 19

VI. Summary and discussion 20

Acknowledgments 21

References 22

*Electronic address: tedkirkp@umd.edu
†Electronic address: dave.thirumalai@gmail.com

I. INTRODUCTION

Glasses, which were created over five thousand years ago in Mesopotamia as objects of astounding beauty, are now used in everyday life. The unusual properties of this amorphous state makes glasses ideal materials for use in myriad ways ranging from displays to architectural solutions to electronics. These applications have literally altered our lifestyles without us fully appreciating their utilities or even being aware of them. Despite their ubiquitous presence the fundamental physics of the process driving their formation has remained elusive (Berthier and Biroli, 2011; Parisi and Zamponi, 2010). The quest to understand the dynamics of the liquid to glass transition has lead to a number of conceptual ideas, which have been used to explain a variety of experimental observations. The unabated efforts to produce a framework to describe the nature of the structural glass transition (SGT) problem have been summarized in a number of reviews in the last twenty years (Berthier and Biroli, 2011; Kirkpatrick and Thirumalai, 1995b; Lubchenko and Wolynes, 2007; Parisi and Zamponi, 2010). In this *colloquium*, we first summarize the essential ideas underlying the random first order transition theory (RFOT) of the glass transition (Kirkpatrick and Thirumalai, 1987a,b; Kirkpatrick *et al.*, 1989; Kirkpatrick and Wolynes, 1987a,b). The RFOT theory, a phrase that was first introduced in (Kirkpatrick *et al.*, 1989), has previously been used to understand both the structural glass transition (Kirkpatrick and Thirumalai, 1995b) as well as various types of spin glass transitions without inversion symmetry (Kirkpatrick and Thirumalai, 1987a,b, 1988b; Kirkpatrick and Wolynes, 1987b). The overarching goal of this work is not to review the current status of theories for glass physics but is to illustrate how the ideas that underlie the RFOT can be used to discuss glassy aspects or features that are manifested in both biological and condensed matter systems. These applications are meant to show case the wide ranging use of ideas that were generated in the physics of the SGT. For lack of space we do not discuss potential connections between the RFOT theory and other interesting subjects such as turbulence (Dauchot and Bertin, 2012, 2013).

A. General remarks on glassy systems

The phenomenology of glasses is well documented. Most liquids, when undercooled rapidly (0.1 - 100 K/min in the laboratory), become extraordinarily viscous (Fig. 1a) over a narrow temperature range. The laboratory glass temperature, T_g, is experimentally defined when the shear viscosity $\eta(T_g) \approx 10^{13}$ Poise (Berthier and Biroli, 2011), which is about fifteen orders of magnitude larger than the viscosity of pure water at room temperature. At T_g the relaxation time becomes so large that thermal equilibrium is not reached in cooling experiments. The dramatic increase in η is not accompanied by discernible changes in the structure. The temperature-dependent relaxation time scale, τ_α ($\approx 1/\eta$), is typically super-Arrhenius, and can be fit using the Vogel-Fulcher-Tamman (VFT) equation,

$$\tau_\alpha = \tau_0 exp[\frac{D}{(T/T_0 - 1)}] \tag{1.1}$$

where τ_0 is a microscopic relaxation time, the parameter D is referred to as the fragility index, and T_0 is a putative ideal glass transition temperature that is obtained by extrapolating measured viscosity data to inaccessible temperatures. Typically α-relaxation, a terminology borrowed from the literature in polymer glasses, refers to motion on length scales larger than the molecular size of the particles. An example of such a fit for salol is given in Fig.1c. The viscosity data have been fit using other forms (Bassler, 1987; Biroli and Garrahan, 2013; Zwanzig, 1988) but here we will assume that Eq.(1.1) provides a good description, which indeed is the case for a number of glass forming materials. As shown schematically in Fig. 1b, for many systems the intermediate scattering function exhibits a plateau after the initial decay before decaying further on the α-relaxation time. The duration of the plateau in regime B (Fig. 1b) increases as the degree of supercooling increases. In addition, the glassy phase is dynamically heterogeneous - a notion that has received considerable attention, and here we argue that this concept, arising naturally from the RFOT, is of great generality. We do not delve into other interesting aberrations in supercooled liquids, such as the break down of Stokes-Einstein relation noted in computer simulations (Barrat *et al.*, 1990; Shi *et al.*, 2013; Thirumalai and Mountain, 1993) and in experiments because they are not relevant to the main themes of this colloquium.

B. Configurational Entropy and the Kauzmann Paradox

Configurational entropy is a key concept in many theories of the glass transition. To define it, consider a free energy functional $F(n, T)$ which depends on number density, $n(\mathbf{x})$, and a temperature, T. We assume that at sufficiently low temperatures $F(n, T)$ has many minima (that is, the number of minima goes to infinity with the system volume, V). These states are labelled by an index γ such that to each valley we associate a free energy F_γ and a free energy density $f_\gamma = F_\gamma/V$. The number of free energy minima with free energy density f is assumed to be exponentially large:

$$\mathcal{N}(f, T, V) \sim \exp[V S_c(f, T)] \tag{1.2}$$

where the function S_c[1] is the configurational entropy or complexity. Physically, it is the entropy arising from an

[1] More precisely this is the definition of the state entropy or complexity. These quantities can be exactly defined in mean-field

assumed exponentially large number of locally stable configurations.

The concept of configurational entropy also plays a central role in experimental glassy physics, especially in the formulation and analysis of the so-called Kauzmann paradox (Kauzmann, 1948), which follows from the following arguments. Below the melting temperature, T_m, the heat capacity $C_p(T)$ of a supercooled liquid is larger than that of the corresponding crystal. As a result of this excess heat capacity, the entropy of the supercooled liquid state is larger than that of the crystal. However, the supercooled liquid state entropy is decreasing faster than the crystal entropy. These observations are illustrated in Fig. 2 and leads to the paradox. If the entropy difference is extrapolated to temperatures below the laboratory glass temperature, T_g, it vanishes at some nonzero temperature called T_K, after Kauzmann. In his original article Kauzmann (Kauzmann, 1948) suggested that the improbable decrease of the entropy of the liquid below that of the crystal phase could be avoided if the barrier to nucleation vanished somewhere between T_g and T_K. Extensive analysis (CA *et al.*, 1986) shows that the crystallization rate slows down more rapidly than the relaxation rate so that Kauzmann's paradox is not realized. One alternative to Kauzmann's suggestion is that a very slowly cooled liquid would continue to lose entropy until, as it approaches the crystal value, an equilibrium phase transition occurs. The nature and the very existence of such a transition has been much debated. Importantly, the extrapolated T_K is always close to the fitted T_0 in Eq.(1.1) (Berthier and Biroli, 2011).

The Adams-Gibbs (AG) (Adam and Gibbs, 1965) theory of the glass transition as well as the RFOT theory (below T_d indicated in Fig. 2) focus on the configurational entropy as defined above. The idea is as follows. Physically, it is reasonable to assume that that the vibrational part of any amorphous state entropy should be more or less equal to the crystal state vibrational entropy. The excess entropy of the liquid state is then attributed to the configurational entropy, S_c. The equilibrium phase transition would occur at T_K when S_c vanishes. In this picture, we expect T_K to equal T_0 because slow transport below T_d is intimately related to loss in S_c. These ideas will be developed in detail below.

Finally, we remark that both AG and RFOT theories lead to the VFT law, Eq.(1.1), via the AG relation,

$$\tau_\alpha = \tau_0 exp[\frac{d}{S_c}] \tag{1.3}$$

with $S_c \sim \epsilon = \frac{T}{T_K} - 1$, vanishing at T_K which is identified as T_0, and d a positive constant. However, the derivations of Eq.(1.3) in the two theories are very different. In the AG theory it is concluded that there is a divergent length scale, $\xi_{AG} \sim 1/|\epsilon|^{1/d}$ while in RFOT the length scale is $\xi_{RFOT} \sim 1/|\epsilon|^{2/d}$. ξ_{RFOT} is derived and discussed further below. The AG correlation length exponent $\nu_{AG} = 1/d$ is in general not consistent with numerous simulations (Berthier and Kob, 2012; Biroli *et al.*, 2008, 2013; Karmakar *et al.*, 2009) to measure correlations in glassy liquids, nor is it consistent with the expected inequality $\nu \geq 2/d$ (Kirkpatrick and Thirumalai, 2014).

C. On the origins of the RFOT

In an attempt to provide a theory to account for the nature of the SGT, a framework was developed in the late 1980s, which was initially inspired[2] by analogies to exotic (explained further below) spin glass models i.e, those without inversion symmetry (Kirkpatrick and Thirumalai, 1987a,b, 1995a; Kirkpatrick and Wolynes, 1987b). From general physical considerations it is logical that there ought to be similarities between structural glasses and spin glasses. A glass, after all, can be thought as a frozen liquid or more precisely flows on time scales that vastly exceed observational time scale (Fig. 1). In both cases there is no obvious long range order. It is only when the systems evolve in time that there are obvious differences. In a liquid a particle can diffuse arbitrarily far away from the initial position as $t \to \infty$, whereas it would be localized in a small region in space in a glass on the observation time scale, τ_{obs} (Fig. 1(d)). Similarly, a spin glass may be thought of as a frozen paramagnet with no long range the magnetic order (Mezard, 1987). When the system develops in time the local magnetic moment points in a specific average direction (a spin at a given time remains correlated with itself at a later time) in the spin glass phase, whereas in the paramagnetic the spin direction averages to zero resulting in the vanishing of local magnetic moment. In both cases, it is only through time evolution can the two phases be distinguished, a concept that will play an important role in our discussion of dynamic heterogeneity.

Despite the compelling analogy between the structural and spin glasses there are also important conceptual differences between the two. First, in SG disorder is quenched (Edwards and Anderson, 1975). In Ising spin glasses the magnetic moments of Mn in an alloy with Ni are permanently frozen. On the other hand, in the SGT problem the randomness is self-generated (Kirkpatrick and Thirumalai, 1989b) as the material is cooled below the melting temperature. Second, there is considerable numerical and experimental evidence for an equilibrium phase transition in three dimensions in Ising spin glasses

and infinite dimensional models. In more realistic systems we identify the complexity with the configurational entropy.

[2] The development was also inspired by an early paper (Kirkpatrick and Wolynes, 1987a) that indicated the MCT of the glass transition is related to a static density functional description of the glassy state.

(Binder and Young, 1986). In the SGT case a thermodynamic transition at $T = T_K \approx T_0$, characterized by a vanishing of configurational entropy, is not universally accepted despite considerable experimental and theoretical support. It is worth emphasizing that the Ising spin glass does not exhibit unusual slowing down in the relaxation times as a liquid that undergoes a transition to a supercooled state. Therefore, an analogy to spin glasses is insightful only if inversion symmetry is not satisfied as is the case in p-spin glass models with $p > 2$ (Gross and Mezard, 1984; Kirkpatrick and Thirumalai, 1987a). Indeed, for such models, we that the mathematical structure of the dynamical equation describing the relaxation of spin-spin correlation for $p = 3$-spin glass model is identical (Kirkpatrick and Thirumalai, 1987a) to the Mode Coupling Theory of the density-density relaxation (Bengtzelius *et al.*, 1984; Goetze, 2009; Leutheusser, 1984). This discovery and subsequent studies linking dynamics and thermodynamics in these exotic mean-field spin glass models to models in which randomness is self-generated lead to the complete formulation of the RFOT (Kirkpatrick *et al.*, 1989). It is worth noting that the Random Energy Model (Derrida, 1981), which does not have a dynamical transition at high temperature, is a special case of p-spin glass model with $p = \infty$ exhibiting one step replica symmetry breaking (Gross and Mezard, 1984).

A valid criticism in using exotic spin glass models to obtain insights into the SGT is that in the former quenched disorder is explicitly modeled in the Hamiltonian whereas in the SGT it is self-generated and manifests itself in the glassy phase. (Because glasses are formed from molecules, whose dynamics (assuming quantum effects are not important) at the microscopic level is Newtonian or Brownian, the information about the self-generated randomness is implicit in the trajectories.) In what we consider, especially in retrospective, to be an important paper (Kirkpatrick and Thirumalai, 1989b), it was shown that the major conclusions drawn based on spin-glass models can be obtained using a model Hamiltonian with short range local order, incorporated using static structure factor, without any need for explicitly modeling quenched disorder. We clarified that the generic ideas within RFOT and related theories that produce a profound connection between static and dynamic description, solely depends on the emergence of an exponential number of metastable states at a dynamical transition temperature, T_d, which is well above T_g, the laboratory glass transition temperature. Moreover, the theory further established that at the so-called temperature Kauzmann temperature, T_K, the entropy associated with the metastable state vanishes resulting in divergence of viscosity Eq.(1.1). Thus, within RFOT $T_K = T_0$, an observation that accords well with many glass forming materials (Berthier and Biroli, 2011).

The body of works created in the late 1980s was subsequently put on firmer foundations by others (Berthier and Biroli, 2011; Mezard and Parisi, 1996; Parisi and Zamponi, 2010). There has also been much discussion about the sense in which the mode coupling theory is a proper mean field theory (Andreanov *et al.*, 2009; Franz *et al.*, 2012; Ikeda and Miyazaki, 2010; Schmid and Schilling, 2010) Very recently (Charbonneau *et al.*, 2013; Kurchan *et al.*, 2013, 2012) all aspects of the RFOT have been illustrated in an exact description of a hard sphere fluid in the limit of high dimensions. We believe these are illuminating studies because they provide a microscopic basis for understanding RFOT theory of the transition of the SGT, which cannot be unequivocally stated for other theories of supercooled liquids and glasses.

D. Assessment of the RFOT

Despite the successes of the RFOT theory of the SGT, some worrying aspects have been raised (Biroli and Bouchaud, 2012), which apparently require further scrutiny. Before addressing these issues briefly, it is worth reminding the readers that although the RFOT theory provides a unified description of both the dynamical transition and the expected thermodynamic transition precipitated by the vanishing of the configurational entropy (Kirkpatrick and Thirumalai, 1987a,b, 1989b; Kirkpatrick *et al.*, 1989) much of the focus has been on the dynamics below T_d. This is a pity because RFOT theory seamlessly integrates the dynamics above and below T_d. With this in mind we address the difficulties raised in (Biroli and Bouchaud, 2012) associated with RFOT. The first is related to the notion of surface tension between two mosaic states, a concept that is relevant below T_d. As we show below, the crucial element in producing the VFT equation with the vanishing of configurational entropy at T_K is that the free energy barriers between mosaic states scale as $\xi^{d/2}$ where ξ diverges at T_K (see below). This implies that there is really no interface between two statistical similar glassy states. Rather, to go from one state to another, roughly $N^{1/2}$ of the N particles in a correlated volume must be rearranged. Consequently, it is our opinion that the issues raised about the surface tension within RFOT merely obfuscates the physics of the activated transitions below T_d. The second point is based on the idea that the free energy barriers might depend on the infinite frequency shear modulus, G_∞ (Dyre, 1998). Such a postulate has no microscopic basis, which relies on the dubious relation that $\eta = G_\infty \tau_\alpha$ (Shi *et al.*, 2013). Therefore, we feel that the Dyre model cannot be compared with RFOT on the same footing. Finally, it has been asserted in (Biroli and Bouchaud, 2012) that the crossover between the liquid like diffusion at $T > T_d$ and the activated transitions below T_d is not only poorly understood but also is without experimental support. This is most certainly not the case as detailed elsewhere (Goetze, 2009). Indeed, unlike the existence of the ideal glass transition temperature, there is much data establishing a change in the dynamics at a temperature far above T_g. Moreover, early computer simulations have

unequivocally established a change in the nature of transport near T_d (Barrat *et al.*, 1990; Mountain and Thirumalai, 1987; Thirumalai and Mountain, 1993). More importantly, using a detailed analysis of experimental data it has been shown (Novikov and Sokolov, 2003) that not only is there ample evidence for the crossover temperature but also the dynamics leading to the crossover may be semi-universal (see below). We conclude that both experiments and simulations have provided compelling evidence for the existence and importance of T_d. In our view the crucial missing point in full support of RFOT is the clear demonstration of the divergent correlation length ξ_{RFOT} at T_K, which was discussed briefly in Section I.B and in more detail below.

II. BASIC NOTIONS OF THE RFOT FOR THE STRUCTURAL GLASS TRANSITION

In this section, we briefly review the basic features of the RFOT as applied to the structural glass transition problem.

A. Two transitions

The important physical aspects of the glass transition and the glassy state that are incapsulated in RFOT (Kirkpatrick and Thirumalai, 1989b; Kirkpatrick *et al.*, 1989) are based on two key ideas. First, the glassy state is essentially a frozen liquid with elastic properties. To describe a glassy state we imagine an order parameter (OP) description in terms of frozen density fluctuations, $\delta n = n - n_l$. Here n is the statistical mechanical average local number density and n_l is the spatially averaged density which is identical to the liquid state density at the same temperature and pressure. In what follows, we will take into account that there can be many glassy states so that n will have a state label, n_s. Other order parameters can be imagined, but frozen density fluctuations are the simplest and are directly related to the most obvious characteristic of a solid: Elastic properties and a non-zero Debye-Waller factor. Because the glassy phase is amorphous or has random characteristics, the frozen density OP is specified by a functional probability measure $DP[\delta n]$ (Kirkpatrick and Thirumalai, 1989b). The first two moments of this measure are,

$$\overline{\delta n(\mathbf{x})} = \int DP[\delta n]\delta n(\mathbf{x}) \tag{2.1}$$

$$q \equiv \overline{[\delta n(\mathbf{x})]^2} = \int DP[\delta n][\delta n(\mathbf{x})]^2. \tag{2.2}$$

Note that because $\overline{n(\mathbf{x})} = n_l$ the density itself cannot be a proper order parameter for the glass transition. In order to capture the essence of the glassy state, something analogous to q must be used (Kirkpatrick and Thirumalai, 1989b; Kirkpatrick *et al.*, 1989).

At the SGT transition the OP will be discontinuous. There are two arguments leading to this conclusion. First, any Landau or LGW type theory for the density n will not have a $n \to -n$ symmetry, and therefore a Landau type theory will lead to some sort of discontinuous transition. More formally, the glassy state is one with a broken translational symmetry, (since it is randomly nonuniform) ,with elastic properties (Palmer, 1982; Szamel and Flenner, 2011). Because of this broken translational symmetry it is impossible to go continuously from a liquid state with time average translational invariance to a glassy state. The second argument imagines that for a given glassy state, the frozen density can be written as (Dasgupta and Valls, 1999; Ramakrishnan and Yussouff, 1979; Singh *et al.*, 1985),

$$n(\mathbf{x}) \sim \sum_i \exp[-(\mathbf{x} - \mathbf{R_i})^\mathbf{2}/2 < (\Delta\mathbf{R})^\mathbf{2} >] \tag{2.3}$$

where the $\{\mathbf{R}_i\}$ are the (random or amorphous) average positions of the particles making up the glassy state and $< (\Delta\mathbf{R})^2 >$ is the average fluctuation of their positions. In the glassy state this is a finite quantity, on the order of a particle diameter, and it determines the Debye-Waller factor and the elastic coefficients of the glass. In a liquid it grows with time and is proportional to the self-diffusion coefficient (Fig. 1d). As the glassy state is approached from the liquid side, it initially grows, but then plateaus on the scale of a molecular diameter. The plateauing of this mean-squared-displacement means that the broken translational symmetry of the glassy state will occur discontinuously. As mentioned earlier, the use of density as an order parameter (Singh *et al.*, 1985) differs conceptually from the ideas of RFOT theory. In the description of the amorphous state using the density functional theory of the liquid to crystal transition (Ramakrishnan and Yussouff, 1979) density itself changes discontinuously near the putative glass transition density for hard sphere systems, whereas in RFOT theory it is the analogue of the Edwards-Anderson order parameter Eq.(2.2), which jumps discontinuously at the ideal glass transition temperature.

The second key idea in the formulation of RFOT is that in general one expects a very large number of distinct metastable glassy states (Goldstein, 1969) . If the number is large enough this in turn leads to two distinct transitions. This is indeed what happens in a many of exactly soluble mean field spin models (Kirkpatrick and Thirumalai, 1987a,b; Kirkpatrick and Wolynes, 1987b; Thirumalai and Kirkpatrick, 1988), in exact high dimensional fluid models (Kurchan *et al.*, 2013, 2012), and in mean-field approximations for a variety of liquid state models (Kirkpatrick and Thirumalai, 1989b). In all of these cases the following scenario is realized. Denote a particular glass state by the label α, with the frozen density in that state given by $n_\alpha = n_l + \delta n_\alpha$ and the free energy in that state equal to F_α. Below a temperature denoted by T_d (the d here stands for dynamical,

cf. below), there are an extensive number[3] of statistically similar states incongruent states (basically uncorrelated) that have zero overlap (Huse and Fisher, 1987):

$$q_{\alpha\alpha'} = \delta_{\alpha\alpha'} q = \frac{1}{V}\int d\mathbf{x}\delta n_\alpha(\mathbf{x})\delta n_{\alpha'}(\mathbf{x}) \tag{2.4}$$

In RFOT it is assumed that these features are also realized in realistic structural glass systems with the only caveat that there is no strict dynamical transition at T_d. Rather, the transition at T_d is avoided but the dynamics changes around T_d signaling the importance of activated transitions.

Because the states are statistically similar one cannot simply use an external field to pick out a particular state. The canonical free energy, F_c, is given by the partition function via

$$Z = \exp[-\beta F_c] = Tr\exp[-\beta H] = \sum_\alpha \exp[-\beta F_\alpha]. \tag{2.5}$$

In the glassy context there are two important cases when F_c is not the physical free energy. First, if the barrier between the states is actually infinite then F_c is not a physically meaningful free energy. Second, if the barriers are finite but the experimental time scale is too short for fluctuations to probe the various states, then it is also not a physical free energy.

A component averaged free energy can be defined by (Bouchaud and Biroli, 2004; Palmer, 1982)

$$\overline{F} = \sum_\alpha P_\alpha F_\alpha, \tag{2.6}$$

with P_α the probability to be in the state α,

$$P_\alpha = \frac{1}{Z}\exp[-\beta F_\alpha]. \tag{2.7}$$

The two free energies, F_c and $\overline{F}$, are related by

$$F_c = \overline{F} + T\sum_\alpha P_\alpha \ln P_\alpha \equiv \overline{F} - TS_c. \tag{2.8}$$

Here S_c, is the configurational entropy (sometimes called the complexity or state entropy), introduced in Section I.B. In general S_c is related to the solution degeneracy and is extensive (and $F_c \neq \overline{F}$) if there are an exponentially large number of states. Note that in infinite range models with a RFOT and a nonzero S_c the physical free energy is $\overline{F}$ because the S_c in Eq. (2.8) is an entropy term which is a measure of parts of state space not probed in a finite amount of time. Since a physical entropy should only be associated with accessible configurations it follows that F_c is not a physically meaningful free energy.

[3] An extensive number of states scales like $\exp(cN)$ for a Nparticle system with c a constant for large N.

The scenario for the two transitions in the RFOT theory can be described as follows. For $T > T_d$ transport is largely not collective, and the topology of state space is unremarkable. However, for $T \to T_d$ the dynamics slows down and the system gets stuck in a glassy metastable state. For $T < T_d$, there are an extensive number of statistically similar, incongruent globally glassy metastable states. If activated transport is neglected these states are infinitely long lived. The liquid state free energy, F_l is lower than the physical glassy state free energy, $\overline{F}$, but it is equal to the canonical free energy, F_c. Because there are so many glassy states, a liquid with probability one will be stuck in one of the metastable glassy states for $T < T_d$. In the absence of activated transport it will remain in that state forever. For infinite range models with an RFOT, exact dynamical calculations shows a continuous slowing down and freezing as $T \to T_d^+$. The same result is also found for some approximate, mean-field like, calculations of dynamics in realistic liquid state models. The transition at T_d is also closely related to the so-called mode coupling theory of the glass transition. In realistic systems, activated transport does take place, and hence on the longest time scales for, $T < T_d$, the dynamics are very sluggish. For this reason T_d is called a dynamical transition: It is a sharp transition only in infinite range models, but in general it sets a temperature region where the dynamics becomes glassy like. In addition, for $T < T_d$ dynamic heterogeneity (DH) plays an increasing important role. This too, can be explained as arising from the multiplicity of states, as we show below.

The driving force for the activated transport in the RFOT scenario for $T < T_d$ is entropic and is given by the state or configurational entropy. At a lower temperature denoted by T_K, after the so-called Kauzmann temperature, the configurational entropy vanishes as does activated transport. In other words, there is a second transition at T_K which is the ideal or equilibrium glass transition temperature. For hard sphere systems for which the volume fraction (ϕ) is the relevant variable the analogues of the two transitions and emergence of other phases as ϕ is increased is schematically shown in Fig.(3).

B. The dynamical transition

1. Theoretical description

The dynamical transition is characterized by the order parameter,

$$q(\mathbf{x}-\mathbf{y},t) = <\hat{q}(\mathbf{x},\mathbf{y},t)> = <\delta n(\mathbf{x},t)\delta n(\mathbf{y},0)>. \tag{2.9}$$

Above T_d this correlation function for fixed $\mathbf{x}-\mathbf{y}$ decays as $t \to \infty$ but as $T \to T_d^+$ its decay gets slower and slower in a power law fashion. The spatial Fourier transform of this quantity is the intermediate scattering function,

$$q(k,t) = <F_{\mathbf{k}}(t)> \tag{2.10}$$

with

$$F_{\mathbf{k}}(t) = \frac{1}{V}\sum_{i=1} e^{i\mathbf{k}\cdot\mathbf{r_i(t)}} \sum_{j=1} e^{-i\mathbf{k}\cdot\mathbf{r_j(0)}}. \quad (2.11)$$

Here $\mathbf{r}_i(t)$ is the position of particle i at time t and V is the system volume.

We illustrate the dynamical behavior of $q(k,t)$ in Fig. (4a) as a function of t for a wavenumber equal to the first peak in the static structure factor, k_{max}. The data are taken from (Kang *et al.*, 2013) a Brownian dynamics simulation of a binary mixture of highly charged spherical colloidal particles, a system that becomes a Wigner glass (Lindsay and Chaikin, 1982) when the fraction of colloidal particles, ϕ, increases beyond ϕ_d the analogue of T_d. In the RFOT description of this system, there is a dynamical transition packing fraction, ϕ_d, as well as an ideal glass transition value, ϕ_K, with $\phi_d < \phi_g < \phi_K$. Because of equilibration problems, the simulations are restricted to ϕ values just past a packing fraction interpreted as ϕ_d because it exhibits all the characteristics of the dynamical transition density for colloidal particles (Kang *et al.*, 2013). The plots show that in the liquid phase $< F_{\mathbf{k}}(t) >$ decays for long times, but as the dynamical transition is approached the system becomes sluggish and $< F_{\mathbf{k}}(t) >$ plateaus for longer and longer times.

A fundamental quantity of interest is,

$$q(t) = \frac{1}{V}\sum_{\mathbf{k}} < F_{\mathbf{k}}(t) > \quad (2.12)$$

At T_d, $q(t)$ no longer decays, except (in non-mean-field models) on the longest times scales. Effectively, it becomes the Edwards-Anderson order parameter for the glass transition:

$$q_{EA} = \lim_{t\to\infty} q(t) \quad (2.13)$$

In RFOT this dynamical order parameter is identical to the equilibrium q given by Eq.(2.2). In other words, equilibrium-like theories are in accord with dynamical theories.

Because the OP involves the square of the density fluctuations it is clear that the associated susceptibility will be something like,

$$\chi_{OP}(\mathbf{x}-\mathbf{y},t) =< \hat{q}(\mathbf{x},\mathbf{y},t)\hat{q}(\mathbf{y},\mathbf{x},t) > - < \hat{q}(\mathbf{x},\mathbf{y},t) >^2 \quad (2.14)$$

Indeed, in (Kirkpatrick and Thirumalai, 1988a) the analog of this quantity was shown to be the relevant susceptibility at a spin glass transition in the RFOT universality class. Also of interest is the spatial and time Fourier transform of $\chi_{OP}(\mathbf{x}-\mathbf{y},t)$,

$$\chi_{OP}(k,\omega) = \int dt \int d\mathbf{x} \exp[-i\mathbf{k}\cdot(\mathbf{x}-\mathbf{y})+i\omega t)]\chi_{OP}(\mathbf{x}-\mathbf{y},t) \quad (2.15)$$

A related susceptibility[4] that is easily measured in simulations has also been defined,

$$\chi_{4|F_k}(t) = \frac{1}{V}\left[< F_k^2(t) > - < F_k(t) >^2\right]. \quad (2.16)$$

In Fig.(4b) we show simulation results for this quantity for the same (Kang *et al.*, 2013) Wigner glass as the dynamical transition is approached. In general, one finds that the location of the maximum and its amplitude grows as the dynamical transition is approached. This correlation function will be further discussed in Section III.

The 'static' susceptibility for the glass transition at T_d is (Kirkpatrick and Thirumalai, 1988a)

$$\chi_{OP}(k) = \lim_{\omega\to 0}\chi_{OP}(k,\omega). \quad (2.17)$$

As $r = T/T_d - 1 \to 0$, the homogeneous susceptibility, $\chi_{OP} = \chi_{OP}(k\to 0)$, in a mean-field theory, diverges as (Kirkpatrick and Thirumalai, 1988a),

$$\chi_{OP} \sim 1/\sqrt{r}. \quad (2.18)$$

At finite and small wavenumber, on the other hand,

$$\chi_{OP}(k) \sim 1/(k^2 + \xi_o^{-2}\sqrt{r}). \quad (2.19)$$

with ξ_o a microscopic (correlation) length. This defines a divergent length scale as $T \to T_d^+$ given by (Kirkpatrick and Thirumalai, 1988a; Kirkpatrick and Wolynes, 1987b) ,

$$\xi \sim \xi_o/r^{1/4} \quad (2.20)$$

This is the same divergence found at a mean-field spinoidol point. It is worth emphasizing again that all of these so-called dynamical results, also follow from the equilibrium theory of the RFOT. It is important to note that they are mean field results for a phase transition that is avoided in realistic systems. Thus, the predicted exponents are effective exponents.

2. Experimental evidence for the dynamical transition

Although there is considerable debate about the existence of $T_k \sim T_0$ there is compelling evidence that the very nature of transport in liquids changes at $T_d > T_g$. In an insightful paper, Goldstein argued forty five years ago that the crossover from liquid like dynamics to transport that involves overcoming free energy barriers (Goldstein, 1969) occurs at temperatures that far exceed T_g. He

[4] The homogeneous order parameter susceptibility is given by $\chi_{OP}(0,t) \sim \sum_{\mathbf{k_1 k_2}}[< F_{k_1}(t)F_{k_2}(t) > - < F_{k_1}(t) >< F_{k2}(t) >$]. For long times this becomes the wavenumber integral of $\chi_{4|F_k(t)}$.

predicted that barrier crossing events start to become important as soon the relaxation time exceeds 10^{-9}s. More recently, by analyzing experimental data of a number of glass forming materials it has been shown that the crossover time is approximately $\tau_c \approx 10^{-7}$s (Novikov and Sokolov, 2003). Remarkably, it was noted that τ_c might be semi-universal. The material-dependent ratio $\frac{T_d}{T_g}$ ranges from 1.1 - 1.7 (see Table 1 in (Novikov and Sokolov, 2003)). As we already pointed out multiple times, T_d roughly corresponds to the temperature predicted by the MCT with the caveat that at T_d the power law singularity describing the dependence of the relaxation time on temperature is avoided in glass forming materials. These crucial studies demonstrate the relevance of T_d in systems without quenched disorder, which invalidate the strict claims made based on the $p = 3$-spin glass model in finite dimensions (Moore and Drossel, 2002).

C. Dynamics and random field effects below the dynamical transition

To a limited extent fluctuations about the RFOT for the SGT have been considered. From our viewpoint the most important aspect of this work has been the establishment of the connection between the SGT problem and the random magnetic field one (Biroli *et al.*, 2013; Franz *et al.*, 2012, 2013) .

The crucial physical point to see this connection, is to realize that for $T < T_d$ ergodicity is broken on all but the longest time scales. This immediately implies that there is a difference between averages over trajectories and averages over initial conditions. In the non-ergodic phase, if time averages over trajectories are first performed than the second average over different initial conditions is analogous to a quenched disorder average. In other words, in the structural glass problem, in the non-ergodic phase, there is self-induced quenched disorder. The local overlap function for two different initial conditions or states (α, β) is,

$$Q_{\alpha\beta}(\mathbf{x}) = n_\alpha(\mathbf{x}) n_\beta(\mathbf{x}) \tag{2.21}$$

with $n_\alpha(\mathbf{x})$ the density in state α. In the high temperature phase the saddle-point solution is $Q^{sp}_{\alpha\beta} = C$ for all $\alpha \neq \beta$. For $T \leq T_d$ there is a simple type of 'replica' symmetry breaking. The order parameter fluctuation $\phi_{\alpha\beta} = Q_{\alpha\beta} - \mathrm{C}$ satisfies the action (Franz *et al.*, 2012),

$$S = S_2 + S_3 + S_4 \cdots \tag{2.22}$$

with S_j of $O(\phi^j)$. The first few terms are,

$$S_2 = \frac{1}{2}\int d\mathbf{x}[\sum_{\alpha\beta}(\nabla\phi_{\alpha\beta})^{\mathbf{2}} + m_1 \sum_{\alpha\beta}\phi^{\mathbf{2}}_{\alpha\beta}$$

$$+ m_2 \sum_\alpha (\sum_\beta \phi_{\alpha\beta})^2 + m_3 (\sum_{\alpha\beta}\phi_{\alpha\beta})^2], \tag{2.23}$$

$$S_3 = -\frac{1}{6}\int d\mathbf{x}\left(w_1 tr\phi^3 + w_2 \sum_{\alpha\beta}\phi^3_{\alpha\beta}\right), \tag{2.24}$$

and

$$S_4 = \frac{1}{4}\int d\mathbf{x}\left(u_1 tr\phi^4 + \cdots\right). \tag{2.25}$$

The mean-field dynamical transition occurs at $m_1 = 0$. It is easily seen that the random field aspects of this action is reflected by the m_2 and m_3 terms in S_2. In particular, to leading singular order all the Gaussian propagators behave as,

$$< \phi_{\alpha\beta}(\mathbf{k})\phi_{\gamma\delta}(-\mathbf{k}) >= \frac{-4(m_2+m_3)}{(k^2+m_1)^2} + \cdots \tag{2.26}$$

That is, it is proportional to a propagator squared, which is characteristic of a random field problem (Nattermann, 1997; Young, 1998) .

The theory given by Eq. (2.22) is a random field problem with cubic terms, which in general reflects the symmetry difference between fluids and most random magnet problems. Interestingly, it has been shown that this theory has a critical point when $w_1 = w_2$ where the cubic term vanishes (Franz *et al.*, 2012).

The implications of this connection of the SGT problem to the random field problem is not completely understood. The arguments are perturbative in nature and seem to neglect the activated transport that takes place for $T < T_d$. Nevertheless, one speculates that some of the features important in random field magnets such as activated scaling are also relevant in the SGT problem.

D. Entropy crisis and divergent activated transport near the ideal glass transition

The RFOT is a new type of discontinuous phase transition. General arguments and exact calculations in infinite range models indicate that a divergent coherence or correlation length exist as an ideal glass transition is approached. Physically, this divergent length is like a finite size scaling length. Generalizing arguments of Fisher and Berker (Fisher and Berker, 1982) for regular first order phase transition to a RFOT gives the correlation length that diverges as [5] $\xi \sim 1/\epsilon^\nu$, with $\epsilon = T/T_K - 1$, and correlation length exponent (Kirkpatrick *et al.*, 1989),

$$\nu = \frac{2}{d}. \tag{2.27}$$

[5] We use $r = T/T_d - 1$ as the dimensionless distance from the dynamical transition and $\epsilon = T/T_K - 1$ as the dimensionless distance from the ideal glass transition.

This result is expected (Kirkpatrick and Thirumalai, 2014) to be exact for all dimensions where a transition takes place. An exact finite size scaling calculation (Kirkpatrick and Wolynes, 1987b) for an infinite range model undergoing an RFOT also gives this value. In this case as $\epsilon \to 0$ the configurational entropy per site vanishes as,

$$S_c/N \sim \epsilon \tag{2.28}$$

and the finite size correlation length diverges as,

$$\xi \sim 1/|\epsilon|^{2/d} \tag{2.29}$$

An important characteristic of a glass transition is the occurrence of extremely long relaxation time scales. While critical slowing down at an ordinary transition means that the critical time scale grows as a power of the correlation length, $\tau \sim \xi^z$ with z the dynamical scaling exponent, at a glass transition the critical time scale grows exponentially with ξ,

$$\ln(\tau/\tau_o) \sim \xi^{\psi} \tag{2.30}$$

with τ_o a microscopic time scale, and ψ a generalized dynamical scaling exponent. Effectively, Eq.(2.30) implies $z = \infty$. As a result of such extreme slowing down, the system's equilibrium behavior near the transition becomes inaccessible for all practical purposes. Thus, realizable experimental time scales are not sufficient to reach equilibrium, and one says the system falls out of equilibrium.

Activated scaling, as described by Eq. (2.30), follows from a barrier picture of the system's free energy landscape. In the context of the structural glass transition it is called the so-called mosaic picture (Bouchaud and Biroli, 2004; Kirkpatrick *et al.*, 1989). The basic idea is that for $T_d > T > T_K$ there is an entropic driving force that causes a compact, glassy state of size ξ^d to make a transition to a different glassy state, with the same approximate free energy, also of size ξ^d. The physical picture that results is a system that looks like a mosaic, or patchwork, of different glassy regions separated by diffuse or fuzzy interfaces slowly making a transition to yet other glassy states. For the uncorrelated states that exist above T_K the law of large numbers (Thirumalai *et al.*, 1989a) is consistent with a barrier that scales like $\sim \xi^{d/2}$. This is also consistent with scaling and an entropic driving force $\epsilon\xi^d \sim \epsilon^{-1}$, if $\nu = 2/d$. In the original RFOT paper (Kirkpatrick *et al.*, 1989), a wetting argument, along the lines proposed for RFIM (Villain, 1985), was given that also led to barriers scaling like $\xi^{d/2}$. All of this in turn implies a Vogel-Fulcher law for the temperature dependence of the relaxation time should hold as the glass transition is approached:

$$\tau \sim \tau_o \exp[\frac{D}{T/T_K - 1}] \tag{2.31}$$

with D a positive constant. Within RFOT and related theories T_K is identified with T_0 in the VTF equation, Eq.(1.1).

As noted in Section I.D that the barriers scaling like $\xi^{d/2}$ implies there is really no interface between two statistical similar glassy states.

III. DYNAMIC HETEROGENEITY, LAW OF LARGE NUMBERS, RARE REGIONS, AND ACTIVATED SCALING IN GLASSY SYSTEMS

A. Dynamic heterogeneity

Experimentally, various spectroscopic techniques have revealed *hetrogeneous* relaxation in glassy systems (Berthier, 2011; Bouchaud and Biroli, 2005; Ediger, 2000) . In such systems, there is non-exponential decay of correlations that can be explained as arising from the superposition of different regions decaying with different relaxation rates.

A large number of molecular simulations have provided visualization of the microscopic details of the dynamical heterogenities in glass forming systems (Donati *et al.*, 2002; Ediger and Harrowell, 2012). These simulations have provided direct evidence of dynamic heterogeneities, i.e., the existence of finite time correlated domains with a length scale that can exceed the molecular scale. An illustrative simulation result is shown in Fig. (5). Experiments to directly visualize these dynamic heterogeneities have also been performed in colloidal glasses.

The chief theoretical construct used to understand dynamic heterogeneity near the dynamical transition is the order parameter susceptibility and the related function $\chi_{4|F_k}(t)$, both of which are defined in Section II.B. In Fig.(4b), we show $\chi_{4|F_k}(t)$ as a function of t for a wavenumber equal to that of the first peak of the static structure factor, k_{max} for a system forming a Wigner glass. In general, one finds that there is a peak that becomes larger and moves to longer times as the glass transition is approached.

Ordinary scaling ideas can be used to partially explain and interpret these results. The simulations show that the location in the peak of $\chi_{4|F_k}(t)$ increases as a power law as ϕ_d is approached from below according to (Kang *et al.*, 2013),

$$t^* \sim (\phi^{-1} - \phi_d^{-1})^{-\gamma_\chi} \tag{3.1}$$

$$\gamma_\chi \simeq 1.05 \tag{3.2}$$

General scaling ideas, on the other hand, give that $t^* \sim \xi^z \sim 1/r^{\nu z}$ with z the dynamical scaling exponent, $r = (\phi^{-1} - \phi_d^{-1})$ is the distance from the dynamical transition, and ν is the correlation length exponent for the dynamical transition. According to the mean-field description in Section II.B, $\nu = 1/4$. This along with Eqs. (3.1) and (3.2) gives $z \simeq 4.2$.This result is consistent with the results of Kim and Saito (Kim and Saito, 2013) .

In non-equilibrium aging simulations and experiments there is a growing, time dependent, correlation length

that has been measured. If we assume ordinary scaling (also see, Section III.D below) to describe the r and t dependence of the correlation length then the natural assumption is,

$$\xi(r, 1/t) = b f_\xi(b^{1/\nu} r, b^z/t) \tag{3.3}$$

with b an arbitrary length rescaling factor and f_ξ a scaling function. Choosing $b = t^{1/z}$ gives,

$$\xi(r, 1/t) = t^{1/z} f_\xi(r t^{1/\nu z}, 1) \tag{3.4}$$

This implies that for $rt^{1/\nu z} < 1$ there is a correlation length that grows in time as $\sim t^{1/z} \sim t^{.24}$.

B. Dynamic heterogeneity and violation of law of large numbers

Ingenious four-dimensional NMR experiments (Sillescu, 1999; Sillescu *et al.*, 2002) and dielectric relaxation measurements have provided the needed evidence for heterogeneous dynamics in glass forming materials. However, much of our understanding of the notion of DH comes from computer simulations, most of which have been quantified using the four-point dynamic susceptibility function. The lack of symmetry breaking as the SGT occurs forces us to use higher order correlation functions to distinguish between the liquid and the glassy phase. Within the RFOT (and MCT) formalism the natural dynamic order parameter is the two-point intermediate scattering function given by Eq. (2.11). It decays to zero in the liquid phase, and acquires a plateau whose duration grows as the extent of supercooling increases Fig.(4a). Thus, it is necessary to use the fluctuations in $F_k(t)$, which plays the role of generalized susceptibility, $\chi_{4|F_k(t)}$, Eq.(2.16), to distinguish between the states accessed above and below T_d (Kirkpatrick and Thirumalai, 1988a) . Although it is physically most meaningful to use fluctuations in $F_k(t)$ a number of studies have used $\chi_{4|S}$ (S is some observable) to infer the nature of dynamical heterogeneity in several model systems (Bouchaud and Biroli, 2005; Dasgupta *et al.*, 1991; Donati *et al.*, 2002; Toninelli *et al.*, 2005) . The four point correlation function $\chi_{4|F_k(t)}$ ($S = F_k$) is the variance in $F_k(t)$. For a large number of systems it is found that $\chi_{4|F_k}(t)$, at a specified k, has a peak in the time-domain with the amplitude that grows with increased supercooling. In Fig.(4b), we show a typical dependence of $\chi_{4|F_k}(t)$ at k_{max} for a Wigner glass for which increasing volume fraction of the colloidal particles is roughly analogous to decrease in temperature. By computing the k-dependence of $\chi_{4|F_k}(t)$ an estimate for the length scale, ξ_{DH}, associated with dynamic heterogeneity (DH length) can be made with the assumption that the maximum amplitude $\chi_{4|F_k}(t)$ follows the Ornstein-Zernicke form, $\chi_{4|k}(t) \approx \frac{\xi_{DH}^2}{(1+(\xi_{DH}k)^2)}$.

A physical consequence of the length scale associated with dynamic heterogeneity is that the usual law of large numbers, which is obeyed in liquids, is violated in the glassy phase (Thirumalai *et al.*, 1989a). The plausible emergence of a natural length scale within which the particles are highly correlated allows us to imagine that the below $T < T_d$ the entire sample can be partitioned into subsamples whose size can be associated with the DH length. As the temperature decreases we expect this length to be large enough that meaningful averages over the number of particle within DH length can be performed. In the liquid phase ($T < T_d$) the statistical properties of the liquid (for example the average energy of particles of a given type) would be independent of the subsample size, and should will coincide with that of the entire sample (within the usual fluctuation effects) provided the DH length is large. This is the usual statement that the law of large numbers is expected to hold in the ergodic liquid phase. On the other hand, in the glassy phase each subsample is likely to be distinct, and consequently there ought to be variations between one subsample to another. Because the time for rearrangement of one subsample to another gets slower and slower as the degree of supercooling increases the in-equivalence between particles of a given type between two samples would persist even on the observation time, τ_{obs}. Thus, no single sub sample can statistically characterize characterize the equilibrium properties of the entire sample, even after suitable time average . In other words, in the glassy phase the law of large numbers is violated, and there are ought to be subsample to subsample fluctuations. Only by examining the entire sample on timescales that far exceed the observation times can these intrinsic heterogeneities between subsamples become irrelevant. This physical picture suggests that DH dynamical heterogeneity a consequence of the emergence of glassy clusters, which are essentially frozen with relaxation time that far exceeds τ_{obs}. Because of the variations in both equilibrium and relaxation properties from subsample to subsample a glassy phase is inherently heterogeneous, as noted in several studies.

These concepts were illustrated using computer simulations of binary soft sphere mixtures (Thirumalai *et al.*, 1989a), and more recently mixtures of charges colloidal particles, which form Wigner glasses at high densities or volume fractions (Kang *et al.*, 2013). This experimentally characterized system is liquid-like at volume fractions ϕ below $\phi \approx \phi_d \approx 0.1$, and turns into a Wigner glass above $\phi > .1$. We divided the simulation sample into subsamples with appropriate size determined by an approximate measure of structural entropy. It order to establish the violation of law of large numbers we showed in Fig.(7) of (Kang *et al.*, 2013) the time evolutions of distribution of the structural entropy, s_3 for a large subsample and the whole sample for $\phi = 0.02$ and $\phi = 0.2$. As expected based on law of large numbers, we found that in the liquid phase ($\phi = 0.02$) the distributions $P(\bar{s_3}|t)$ are almost the same for all t values that exceed the typical relaxation time. In contrast, at higher volume fractions ($> \phi_d$) where ergodicity is effectively broken, the $P(\bar{s_3}|t)$

for the subsample are substantially different from that of the entire sample, thus violating the law of large numbers . Because different subsamples behave in a distinct manner and do not become equivalent, we surmise that dynamical heterogeneity is a consequence of violation of law of large numbers. It should be noted that only by examining the time evolution of the subsamples in the liquid and the glassy phase can this link be established. The intuitive arguments given here are made more precise in the following section.

C. Rare region dynamics near the glass transitions

The existence of DH suggests that in a very viscous liquid the longest time decay of any time correlation function will be determined by the large rare region or anomalous clusters of particles of some linear dimension L (Berthier, 2011) . These large clusters are fluidized and can relax to a more typical configuration of particles in some characteristic time $\tau(L)$. For this argument to be sensible L must be larger than a molecular scale. To estimate the effect of these large rare regions on a typical time correlation function an average over L must be performed.

Since the large clusters are rare, we assume that their probability distribution is controlled by Poisson statistics so that the tail probability of an unusual cluster of size L is[6] ,

$$P(L) \sim \exp(-cL^d) \tag{3.5}$$

with c a positive constant. We also assume that a typical correlation associated with the rare region decays exponentially as,

$$C(L,t) \sim \exp[-t/\tau(L)]. \tag{3.6}$$

It is also reasonable to assume that the long time dynamics of these fluidized regions is diffusive so that $1/\tau(L) \to Dk^2 \to D(L)/L^2$. We consider two temperature regions. The first is appropriate for temperatures near T_d and the second for temperatures close to T_K or the laboratory glass transition temperature, T_g.

In the first region the scale dependence of D is ignored so that the average correlation function decays as,

$$C(t \to \infty) \sim \int dL \exp[-cL^d - Dt/L^2]$$

$$\sim \exp[-A(Dt)^{d/(d+2)}] \tag{3.7}$$

with A a positive constant. The characteristic length scale $L_1^*(t) \sim [Dt]^{1/(d+2)}$. Equation (3.7) is the stretched exponential behavior typically observed in correlation functions in simulations near T_d with a large time, τ, scale given by $\tau \sim 1/D$. For example, the solid lines in Fig.(4a) are a fit to a stretched exponential $\sim \exp[-(t/\tau)^\beta]$ with $\beta = 0.45$. In general a distribution of relaxation times, $P(\tau)$, can be defined by writing

$$C(t) \sim \int d\tau P(\tau) \exp[-t/\tau]. \tag{3.8}$$

By comparing Eq. (3.7) and Eq. (3.8) it follows that,

$$P(\tau \to \infty) \sim \exp[-(D\tau)^{d/2}], \tag{3.9}$$

with a tail that decays faster than exponential.

In the second, lower temperature, region, the scale dependence of the diffusion constant becomes most important. If we assume that $D(L)$is inversely proportional to the RFOT relaxation time,

$$\tau(L) = \tau_m \exp[aL^{d/2}] \tag{3.10}$$

with τ_m a microscopic time and a a positive constant. Using all of this an average correlation function then decays for long times as,

$$C(t) \sim \int dL \exp[-cL^d - (t/\tau_m)(e^{-aL^{d/2}}/L^2)]$$

$$\sim \exp\{-A[\ln(t/\tau_m)]^2\} \tag{3.11}$$

with A a positive constant. The conclusion is that for long times $C(t)$ decays faster than any power law, but slower than any stretched exponential. The characteristic length scale for this case is $L_2^*(t) \sim (\ln t)^{2/d}$.

In this case, the distribution of relaxation times, $P(\tau)$, is given by,

$$P(\tau \to \infty) \sim \exp\{-c[\ln(\tau/\tau_m)]^2\} \tag{3.12}$$

with a characteristic tail that decays slower than any exponential.

Finally we note that in a given system well below T_d there will be an intermediate time region where the scale dependence of $D(L)$ is not important and a stretched time behavior will be observed, before crossing over to the exponential of $[\ln t]^2$at the longest times. The crossover time will be roughly given by the equation $L_1^*(t) \sim L_2^*(t)$.

D. Activated scaling near the glass transition

Activated scaling was developed to understand finite dimensional (three dimensions) spin glasses and random field magnets where the dynamics is controlled by large, possibly divergent, free energy barriers (Fisher and Huse, 1988). Similar ideas can be applied to the structural glass problem, also in three-dimensions.

[6] Although related, this assumption is physically distinct from what is used in quenched disordered systems (Vojta, 2006). Here we simply postulate that since the events are rare, they are controlled by a Poisson distribution.

Here, we examine the behavior of the glass transition susceptibility, introduced in Sec II.B using activated scaling ideas (Fisher and Huse, 1988) as the ideal glass transition is approached. We start with the observation that the first order nature of the ideal glass transition implies that the scale dimension of $q(\mathbf{x},t)$ is zero. This and the activated scaling ansatz gives that the wavenumber and time dependent glass transition susceptibility will satisfy the scaling law,

$$\chi_{OP}(\epsilon,k,t) = b^d F_\chi[\epsilon b^{1/\nu}, bk, \frac{b^{d/2}}{\ln(t/t_o)}] \tag{3.13}$$

where $\epsilon = T/T_K - 1$ is the dimensionless distance from the ideal glass transition, t_o is some microscopic time scale, and F_χ is a scaling function. Note that we have used here that the barrier height scales as $b^{d/2} \sim \xi^{d/2}$. This equation implies a number of non-trivial results. For example, at zero wavenumber, and at the ideal glass transition temperature we can choose $b = [\ln(t/t_o)]^{2/d}$ to obtain,

$$\chi_{OP}(0,0,t\to\infty) \sim [\ln(t/t_o)]^2. \tag{3.14}$$

This dynamic scaling result is valid as long as $\epsilon \ln(t/t_o) < 1$. It also defines a dynamic crossover ϵ being given by,

$$\epsilon_x \sim 1/[\ln(t/t_o)] \tag{3.15}$$

Physically this means that the large correlations that exist at T_K can be measured by examining the slow growth in time of the glass transition susceptibility around $k = 0$. This should be experimentally relevant. If the exponent of 2 in Eq.(3.14) can be experimentally demonstrated then it would be very strong evidence for the validity of the RFOT theory of the SGT.

The frequency dependent glass transition susceptibility defined by Eq.(3.14) can similarly be expressed as a scaling function. In general the ϵ_x given by Eq.(3.15) will give the scale distinguishing static critical behavior from dynamical critical behavior for all quantities as $T \to T_K$.

Although not as rigorously founded as the scaling law for χ_{NL}, we can also give a scaling law for the frequency dependent shear viscosity, $\eta(\epsilon,\omega)$. Because $\eta(\epsilon,\omega)$ is related to a time integral of a time correlation function its static value is proportional to τ given by Eq. (2.30). We then obtain,

$$\eta(\epsilon,\omega) = \exp(b^{d/2}) F_\eta[\epsilon b^{1/\nu}, \frac{b^{d/2}}{\ln(1/t_o\omega)}] \tag{3.16}$$

with F_η a scaling function. The static or zero frequency shear viscosity then behaves as τ but for $\epsilon < 1/\ln(1/t_o\omega)$ it behaves as

$$\eta[\epsilon \ln(1/t_o\omega) < 1] \sim \frac{1}{t_o\omega}. \tag{3.17}$$

Again, the important physical and experimental point is that ϵ_x, given by Eq.(3.15), sets the crossover scale in either time or frequency ($t \to 1/\omega$) space. Note that η being simply proportional to τ in Eq.(3.16) is needed to obtain Eq.(3.17), which in turn is required for the proper stress/strain relation in the glassy phase.

Following Section III.A we next use activated scaling ideas to describe the time-dependent aging correlation length. In this case the natural assumption is,

$$\xi(\epsilon,1/t) = bF_\xi(b^{1/\nu}\epsilon, e^{b^{d/2}}/t) \tag{3.18}$$

with F_ξ a scaling function. Choosing $b^{d/2} = \ln t$ and using $\nu = 2/d$ gives,

$$\xi(\epsilon,1/t) = (\ln t)^{2/d} F_\xi(\epsilon \ln t, 1) \tag{3.19}$$

Thus, we expect that close to the ideal glass transition and for $\epsilon \ln t < 1$, there ought to be a correlation length in aging experiments that grows as $\sim (\ln t)^{2/3}$ in ($d = 3$).

IV. UNDERSTANDING BIOLOGICAL PROBLEMS FROM THE PERSPECTIVE OF GLASS PHYSICS

There are several ways in which concepts in glass physics can be used to understand many aspects of biological systems. At the cellular level, on length scale on the order of μm, functions are carried out often by several interacting biological molecules. Transport in eukaryotes, supporting cytoskeletal structures, is powered by ATP-driven motors. However, in *E. Coli.* all dynamical processes occur by diffusion. Moreover, the dynamics has to occur in a heterogeneous crowded environment within a restricted time interval with the upper bound being the cell doubling time. Therefore, it is likely that the biological molecules only sample a restricted part of the access conformational space, which implies that ergodicity could well be broken as in a liquid undergoing glass transition. On longer length scales, involving communication between cells, needed in diverse phenomena such as development and wound healing, there are manifestation of glass like behavior or at least evidence of highly heterogeneous behavior (Altschuler and Wu, 2010; Herms *et al.*, 2013; Pelkmans, 2012). This is not entirely surprising because these processes involve collective movements, which can be sluggish. In particular, in tissues without gaps between cells there is evidence that the collective dynamics (Angelini *et al.*, 2011), much like correlated movements of particles in the glassy state, have many of the hall marks of the SGT (Garrahan, 2011). Here, we use a few examples to illustrate that concepts in glass physics, which at first glance may seem unrelated to biology, are useful in providing insights into dynamics in biological systems from nm to μm, and beyond.

A. Countable number of structural states in the sequence space of proteins

An astounding aspect of proteins and RNA is that natural foldable sequences, whose number is much smaller

than all possible sequences, self-organize themselves spontaneously often without the help of molecular chaperones (Dill *et al.*, 2008; Onuchic *et al.*, 1997; Schuler and Eaton, 2008; Shakhnovich, 2006; Thirumalai *et al.*, 2010). Why are the number of structure forming sequences so small? Answering this question quantitatively forces us to think in terms of partitioning of the vast sequence space in terms of disjoint states (just as described in Section (IIA)). By envisioning the partitioning of both the sequence and conformational space of proteins and RNA in terms of the associated landscapes, we can begin to appreciate the emergence of structures as well as the characteristics of sequences that make them biologically viable, implying that they fold relatively rapidly.

Here, we only consider proteins. The primary building blocks of proteins are α-helices (one dimensional ordered structures), β-sheets (contain two dimensional order), and loops of varying bending rigidity (Stryer, 1988). From these seemingly simple building blocks (referred to as secondary structural elements) a large number of three dimensional structures can be constructed. The number of distinct topological folds is suspected to be only on the order of a few (at best) thousand,- a relatively small number (Chothia, 1992). How do these preferred folds, which should also be kinetically accessible on biologically relevant time scale, emerge from the dense sequence space? The number of sequences of a polypeptide chain with N amino acids is 20^N, which is astronomically large even when N takes on a modest value. It is likely that only an extremely small fraction of the sequences encodes for the currently known protein structures. A quantitative mapping between sequence space and structures, obtained using lattice models (Li *et al.*, 1996), shed light on the structure of the sequence space landscape. In order to appreciate the partitioning of the sequence space it is worth recalling that natural proteins in their native states are (i) compact, and (ii) dense interior is made up of predominantly hydrophobic residues. With these two restrictions on the native structures, it has been shown that even though the number of sequences is astronomically large, the number of compact low energy structures (protein-like) is considerably smaller both in two and three dimensions (Camacho and Thirumalai, 1993b; Lin and Zewail, 2012; Thirumalai and Klimov, 1999). This would imply that for many sequences the low energy compact structures could be nearly the same, as was beautifully illustrated by exploring sequences in a three dimensional lattice model (Li *et al.*, 1996). In other words, the basins of attraction in the structure space are rare enough so that a large number of sequences map on to precisely one basin, thus explaining the emergence of greatly limited number of structures from the sea of sequence space (Chothia, 1992).

Similar considerations hold for RNA with the crucial difference that RNA structures are lot more degenerate compared to proteins (Thirumalai *et al.*, 2001). An identical RNA sequence can fold into two distinct structures performing entirely different functions (Schultes and Bartel, 2000). This implies that the sequence space landscape could be multiply connected with larger number of structurally degenerate states compared to proteins. From the perspective of navigating the sequence space landscape, which presumably occurs on the evolutionary time scale, the dynamics is predicted to be slower than evolvability of protein sequences.

B. Kinetic accessibility and folding rate dependence of proteins and RNA on N

A corollary of the finding that natural sequences fold into minimum energy compact strctures quickly is that random sequences cannot exhibit protein-like behavior both on account of stability and perhaps more importantly kinetic accessibility of the folded states (Bryngelson and Wolynes, 1989). Even if random heteropolymers formed by covalently linking various amino acids have unique ground states the folding dynamics would be highly sluggish (Takada *et al.*, 1997; Thirumalai *et al.*, 1996) such that deleterious aggregation could intervene before folding. A solution to this conundrum is that the folding transition temperature, T_F, of sequences that lead to functional proteins should exceed the equilibrium glass transition temperature, a suggestion that was based on the extension of the Random Energy Model (REM) to protein folding with the native state playing a special role (Bryngelson and Wolynes, 1989). In the REM, equivalent to p-spin model with $p \to \infty$, there is an entropy crisis at a finite temperature. Because of finite size of proteins there is no strict entropy crisis, and hence it was realized that T_F has to exceed a dynamic glass transition temperature, T_g, for folding to the native state to occur in biologically meaningful time (Socci and Onuchic, 1995). Ideas based in polymer physics further showed that the interplay of T_F, and the equilibrium collapse temperature (T_θ) (Camacho and Thirumalai, 1993a) could be used to not only fully characterize the phase diagram of generic protein sequences but also determine their foldability, a prediction that has been experimentally validated only very recently (Hofmann *et al.*, 2012). Based on the study of dynamics of random copolymer models it was proposed that the upper bound on $\frac{T_F}{T_{gd}}$ is $\frac{T_F}{T_\theta}$ (Thirumalai *et al.*, 1996). Thus, by studying disordered systems exhibiting glassy behavior insights into foldable sequences were obtained.

The description of activated dynamics using RFOT was also adopted to obtain an estimate of the dependence of the folding rates of globular proteins on N. The folding reaction typically involves crossing a free energy barrier, and hence the folding time is given by $\tau_F = \tau_0 e^{\Delta F^\ddagger / k_B T}$ where $\Delta F^\ddagger$ is the average free energy separating the native state from an ensemble of partially structured and compact states. The scaling of $\Delta F^\ddagger$ with N parallels the arguments developed in the context of activated dynamics using RFOT concepts (Thirumalai, 1995). We assume that the free energy distribution of the low energy struc-

tures is given by a Gaussian distribution, which is also consistent with computations on model glass forming systems. Since there is an ensemble of independent transition states connecting the conformations of compact but non-native states and the native state it is natural to assume that the barrier height distribution is also roughly Gaussian with a dispersion $\langle \Delta F^2 \rangle$ that scales as N. Since the barrier height distribution is essentially a Gaussian it follows that $\Delta F^{\ddagger} \approx \langle \Delta F^2 \rangle^{1/2} \approx \sqrt{N}$. This physically motivated argument is also consistent with the tenets of RFOT. For proteins the appropriate length scale is essentially the whole protein molecule, and hence

$$\Delta F^{\ddagger} \approx N^{\frac{1}{\nu d}}, \tag{4.1}$$

and with $\nu = 2/d$ we obtain the important result that the barrier to folding scales sub linearly with N. This scaling type relation has been successfully applied to rationalize the folding rates of a large number of proteins whose folding rates cover seven orders of magnitude (Fig. 6a).

Although Eq.(4.1) explains the data for proteins, we expect that the theory should account for the folding rate changes with the number of nucleotides (N) even better because RNA has multiple folded metastable states (Thirumalai and Hyeon, 2005), which could be thought of as free energy excitations around the native state. It is also likely that even the functional state for RNA may not be unique (Solomatin *et al.*, 2010), thus [7] making the energy landscape very much glass like. In accord with this expectation, it has been found that the folding dynamics is sluggish with trapping in metastable states occurring with high probability (Pan *et al.*, 1997). As a consequence of the highly rough free energy surface the folding rates can be predicted using Eq. 4.1. Remarkably, the folding rates of RNA also obeys $\tau_F = \tau_0 e^{\sqrt{N}}$ with high accuracy with $\tau_0 \approx 1\mu$s (Fig. 6b).

C. Persistent heterogeneity

The underlying energy landscapes of biological molecules, especially large RNA, are rugged consisting of multiple states that are separated by large barriers. As a consequence, it is most likely the case that they should exhibit glass-like behavior, which has only been recently revealed most clearly using single molecule experiments although pioneering experiments by Frauenfelder (Frauenfelder *et al.*, 1988) had already anticipated these possibilities. An important consequence of several studies is that the functionally competent states of RNA and possibly proteins may not be unique, as is generally assumed. In terms of the RFOT description of glasses it implies that there are many components or states in the folding landscape and just as in glasses the canonical free energy is not relevant as would be the case if the folded state did always correspond to the global free energy minimum (Anfinsen and Scheraga, 1975). The widely accepted notion that the native state of proteins and RNA are unique was inferred using bulk ensemble experiments tacitly assuming that ergodicity is established on τ_{obs}. In a rugged landscape, a specific molecule with an initial conformation distinct from others only samples limited conformational space corresponding to a single state. Ergodically sampling all states would only be possible on time scales longer than biologically relevant times. This scenario results in heterogeneous dynamics as in glasses, and ensemble average would obscure the complexity of the structural features of the underlying landscape. Indeed, recent findings from single molecule experiments on several biomolecular systems explicitly showed persistent heterogeneities in time traces (or molecule-to-molecule variations) generated under identical folding conditions (Borman, 2010; Ditzler *et al.*, 2008; Okumus *et al.*, 2004; Solomatin *et al.*, 2010; Zhuang *et al.*, 2002). Unlike phenotypic cell-to-cell variability among genetically identical cells, which can be visualized using microscope (Pelkmans, 2012), the observation of heterogeneity among individual biomolecules on much smaller length scales is tantalizing because it would make it difficult to reconcile this concept with the conventional notion that functional states of proteins and RNAs are unique or that various native basins of attraction easily interconvert on the time scale of observation. For example, in docking-undocking transitions of surface immobilized hairpin ribozyme (Zhuang *et al.*, 2002) and *Tetrahymena* group I intron ribozyme (Solomatin *et al.*, 2010), time traces for individual molecules display very different dynamic pattern with long memory without apparent compromise in catalytic efficiency. Based on these observations it was suggested that these ribozymes have multiple native states (Solomatin *et al.*, 2010). If this were the case then it follows from the analogies to glasses that (1) the underlying folding landscape must contain multiple discernible states with little possibility of interconversion among them on τ_{obs} implying that ergodicity is effectively broken; (2) the dynamics within each state or basin of attraction ought to be different, which would be a manifestation of dynamic heterogeneity. Demonstrating these important aspects of molecule-to-molecule variations resulting in persistent DH using ensemble experiments is difficult. However, single molecule experiments analyzed using glass physics concepts have recently have shown that these conclusions are indeed valid. We use two completely unrelated examples to illustrate the concept persistent heterogeneity in biological systems at a molecular scale.

Holliday junctions: Holliday Junctions (HJs) are essential intermediates for strand exchange (Fig. 7a) (Lushnikov *et al.*, 2003) in DNA recombination. HJs exist in two distinct isoforms (*isoI* and *isoII*) both of which

[7] There is evidence that in some cases it is likely that even in proteins the folded state may be metastable, especially in the case of mammalian prions (Baskakov *et al.*, 2001; Thirumalai *et al.*, 2003)

have the characteristic X-shaped architectures at high Mg^{2+} concentrations ($\sim$ 50 μM). Using smFRET experiments (Schuler and Eaton, 2008), and concepts from glass physics (Kirkpatrick and Thirumalai, 1989a; Thirumalai *et al.*, 1989b) and complementary clustering algorithms (Sturn *et al.*, 2002; Tamayo *et al.*, 1999) the state space structure and associated dynamics were quantitatively analyzed (Hyeon *et al.*, 2012). Although the HJ dynamics at the ensemble level shows fluctuations between only two-states, trajectories from smFRET reveal a much richer structure with the associated dynamics exhibiting some of the hallmarks associated with glasses. In smFRET experiments efficiency of energy transfer as a function of t is calculated from the measured donor (D) ($I_{D,i}(t)$) and acceptor ($I_{A,i}(t)$) emission intensities as, $E_i(t) = I_{A,i}(t)/(I_{A,i}(t)+I_{D,i}(t))$. Thus, smFRET experiments provided time-dependent "trajectories" in terms of the collective variable, $E_i(t)$, for the i^{th} molecule (Fig. 7b). When an ensemble average over a sufficiently large number of molecules and time $\tau_{obs} \approx 40$ sec is performed one observes a simple two-state behavior (right side of Fig. 7b).

However, detailed analysis of the FRET trajectories revealed surprising evidence of DH. For a given time trace corresponding to a specific molecule α, $\mathcal{T}_{obs} \approx 40$ sec is long enough to observe multiple isomerization events between *isoI* and *isoII* the conformations (Hyeon *et al.*, 2012). The time scale for single isomerization between *isoI* and *isoII* ($\tau^{\alpha}_{\mathrm{I}\leftrightarrow\mathrm{II}}$) is much smaller than $\mathcal{T}_{obs}$ ($\tau^{\alpha}_{\mathrm{I}\leftrightarrow\mathrm{II}} \ll \mathcal{T}_{obs}$) (Fig. 7a and Fig. 8a). Thus, HJ explores the conformations in only the α state exhaustively as shown by the ergodic measure in the upper part of Fig. 8b); however it is not long enough for interconversion to take place between molecules α and β, i.e., $\mathcal{T}_{obs} \ll \tau^{\alpha\leftrightarrow\beta}_{conv}$ where $\tau^{\alpha\leftrightarrow\beta}_{conv}$ is the interconversion time between α and β states, implying that a substantially high kinetic barrier separates the states α and β. In this sense, the kinetics is glassy. Therefore, dynamics of HJs are effectively ergodic within each state on $\mathcal{T}_{obs}$, but $\mathcal{T}_{obs}$ is not long enough to ensure ergodic sampling of the entire conformational space − a situation that is reminiscent of ergodicity breaking in supercooled liquids (Thirumalai *et al.*, 1989b).

How many ergodic components states, which do not interconvert among themselves on $\mathcal{T}_{obs}$, are needed to fully account for the experimental data? In order to determine the number of states K-means clustering algorithm was used to partition the conformational space of HJ into multiple "ergodic subspaces". This was achieved by partitioning the stationary distribution of FRET efficiencies, $p_s(E;i) = \lim_{t\to\mathcal{T}_{obs}} p(E,t;i)$, into distinct states with the requirement that the HJ should ergodically explore the conformational space within each state. At high Mg^{2+} (50 mM) there are five disjoint states (Fig. 8b). The effective ergodic diffusion constant D_E in E-space associated with each state varies greatly from one ergodic subspace to another (Fig 8b).

The HJ gets trapped in one metastable state, which is solely determined by the initial Mg^{2+} binding (Hyeon *et al.*, 2012). In this sense, Mg^{2+} plays the role of a random field, which quenches the conformation of the HJ into one ergodic component. Transition to another ergodic component can be triggered by using an annealing protocol in which the Mg^{2+} concentration is first decreased for a period of time enabling the HJ to explore an entirely different region of the energy landscape. Subsequent increase of Mg^{2+} concentration results in HJ exploring other ergodic components. The redistribution of population is clearly shown in Fig.8c along with the network of connected states. It is indeed surprising that such a small system exhibit all the key hall marks of slow dynamics involving multiple ergodic components.

RecBCD Helicase: Another example (Liu *et al.*, 2013) that vividly illustrates significant molecule-to-molecule variations is in the function of RecBCD helicase in *E. Coli.*, which is involved in the repair of breaks in the double stranded DNA (dsDNA) in an ATP-dependent manner. Here again single molecule experiments showed that there are dramatic variations in the unwinding speed of dsDNA depending on the molecule even though all the enzymes were prepared with no heterogeneity in protein composition. The unwinding velocity, for specified concentration of ATP, can vary greatly as shown in the top panel of Fig. 9. The most likely explanation is that the functional landscape is highly heterogeneous with multiple states each with its own unwinding velocity. This possibility, reminiscent of the phase space partitioning into ergodic subspaces in Holliday Junction, was demonstrated using an ingenious set of experiments. The authors (Liu *et al.*, 2013) examined the possibility that upon initially binding Mg^{2+}-ATP the enzyme is pinned to one the accessible states in the functional landscape. In an initial experiment, they measured the unwinding velocity by incubating the enzyme in the presence of the ligand, and discovered that RecBCD processively unwinds a large portion of DNA at a speed that is "set" by the initial state. Subsequently, they moved the enzyme to a chamber without the ligand to stop unwinding for a period of time of about 20 sec. After the period of inactivity, the complex was supplied with ATP to resume function. Remarkably, the unwinding velocity of the same molecule changed drastically before and after being depleted of Mg^{2+}-ATP, as shown in the bottom panel of Fig. 9. From the perspective of multiple functional states used to understand the dynamics of Holliday junction, we can draw three generic lessons for heterogeneity of RecBCD helicase: (1) The whole space of conformations partitions into distinct subspaces. The observations that the unwinding velocity is determined by the dynamics within a single space implies without changing even after tens of hundreds of base pairs are ruptured, suggest that the enzyme likely ergodically explores conformations within a single state. (2) Transitions between distinct states, with variations in unwinding velocity, can only be achieved by resetting the ATP concentration, which is reminiscent of Mg^{2+} pulse experiments used to estab-

lish interconversion between distinct states in HJ (Hyeon *et al.*, 2012). In both cases, ligands act to quench the conformation to a single substate. Thus, in these systems biological systems heterogeneity is realized by binding of ligands to the biological molecule. As a result of pinning the HJ or RecBCD to a single state ergodicity is effectively broken.

D. Cellular dynamics

Just as is the case in the dynamics of enzymes and ribozymes discussed above, ensembles averages hide the rich dynamics associated with cell-to-cell variations. Although the sources of such variations are hard to pin point except generically as arising from biochemical noise, as is the case in signaling networks, there is virtually no question that such variations are manifested in phenotypes (Almendro *et al.*, 2013; Altschuler and Wu, 2010). Hence, such stochastic variations are of fundamental importance both from the perspective of physics as well as biology. In many studies the behavior of subpopulation of cells are found to be drastically different from the mean characteristics of the ensemble (Altschuler and Wu, 2010), a situation that is hauntingly similar to DH in glasses. There are now countless examples of cellular heterogeneity, but here we focus on one example set in the context of cancer (Almendro *et al.*, 2013). There are apparently profound implications of the observed heterogeneity including possible variations in the treatment of specific cancers as it evolves towards metastatic disease - a topic that is far beyond the scope of the present discussion. We will focus on the similarities between evolution of cells within a single tumor and particulate glasses.

The variability in cells within tumors differing in the ability to metastasize and response to drugs were reported long ago (Heppner and Miller, 1983). Such variations could arise due to genetic heterogeneity but more recently it has been appreciated that non-genetic factors including stochastic variations due to differences in the biochemical reactions, controlling signaling networks, between cells could also contribute to cellular heterogeneity (Fig. 10). This has also been demonstrated most vividly in the differential response of identical cancer cells to drugs (Cohen *et al.*, 2008; Spencer *et al.*, 2009) or other therapies. By carefully measuring the expression levels and locations of a large number of proteins upon treatment of cancer cells with a drug it was shown that there are dramatic variations in the dynamics of certain subset of proteins between cells, resulting in the heterogeneous response. There are substantial variations in the internal stochastic fluctuations within cells, which manifest themselves as differences between cells in their response to a cancer drug. In terms of glass concepts this implies that the various cells can be partitioned (depending on the the dynamics of individual cells as depicted in Fig. 2A in (Cohen *et al.*, 2008)) into distinct states with distinct dynamics as shown by huge variations in YFP intensities among different cells. The similarities to time averaged variations in FRET efficiency between molecule-to-molecule in Holliday Junction is breath taking.

V. GLASS TRANSITION CONCEPTS AND THE RFOT IN CONDENSED MATTER PHYSICS

Typical glassy behavior such as long relaxation times, memory of history, and physical aging are often observed in the electronic and conductance properties of low temperature condensed matter systems (Ovadyaha, 2006; Pollack and Ortuno, 1985). There is an enormous amount of experimental and theoretical work on the glassy behavior in disordered insulators and Coulomb glasses (Amir *et al.*, 2011; Pollack *et al.*, 2013). More recently it has been appreciated that glassy behavior also occurs in disordered metallic systems, or electron liquids. For example, below we discuss some aging experiments in an *metallic* $2D$ MOSFET system. In this system as well as others, see for example the transport properties in the metallic ferromagnet $Sr_{1-x}La_xRuO_3$ (Kawasaki *et al.*, 2014), typical liquid-like glassy behavior is observed.

It is physically very plausible that a strongly correlated disordered electron liquid should have many things in common with classical liquids exhibiting a SGT. First, at least within the RFOT theory of the SGT, the absence or presence of quenched disorder is not important. Second, they are both strongly correlated, frustrated fluids, with identical spatial symmetries. The frustration in general leads to a rugged energy landscape where concepts such as the Kauzmann transition can play a role. In this Section we discuss some connections between the disordered and interacting electron problem and the SGT problem.

We then discuss some theoretical and experimental aspects of super solids and their connection to what has been referred to as a super glass (Kim and Chan, 2004; Ray and Hallock, 2009; Reppy, 2010). Interestingly, the ground state of a interacting Bose system has been related to the Boltzmann measure of a classical hard sphere fluid where RFOT is directly applicable.

Although we focus here on low temperature or quantum condensed matter systems, there are also very interesting classical or higher temperature glassy condensed matter systems. For example, recent experiments (Sato *et al.*, 2014) in charged cluster glasses have shown a remarkable similarity between these systems and viscous liquids. Interestingly, as in RFOT there seems to be an intrinsic relation between dynamics and structure. Related theoretical work based on RFOT ideas is in (Schmalian and Wolynes, 2000).

A. Aging in quantum glassy systems

In general, if $S(t)$ is an observable, or an operator whose quantum average is an observable, at time t and

$h(t)$ is a field conjugate to $S(t)$ than the correlation function C and the response function R,

$$C(t,t') =< S(t)S(t') > \tag{5.1}$$

$$R(t,t') = \frac{\partial < S(t) >}{\partial h(t')} \tag{5.2}$$

are related by a fluctuation-dissipation theorem. In addition, in equilibrium they are functions only of the time difference, $\tau = t - t'$. In a glassy system, the relaxation is often so slow that on an experimental time scales neither of these features hold. Let us define $t = \tau + t_w$ and $t' = t_w$. The time t_w is called the aging time, and it physically represents the duration for which the system was perturbed before allowing it to relax back to an original equilibrium state. In non-glassy systems time correlation and response functions do not depend on t_w. In all glassy systems, on the other hand, this history or aging dependence is ubiquitous (Bouchaud *et al.*, 1997; Struik, 1977).

Next one imagines that $C(\tau+t_w,t_w)$ and $R(\tau+t_w,t_w)$ consist of two parts: A stationary (ST) part that depends only on τ as in non-glassy systems, and an aging (AG) part that depends on the aging time. For example, we write

$$R(\tau + t_w, t_w) = R_{ST}(\tau) + R_{\rm AG}(\tau + t_w, t_w) \tag{5.3}$$

In general, the precise dependence on the aging time is complicated. However, deep in the glassy phase there does appear to be a simple τ/t_w scaling. That is,

$$R_{AG}(\tau + t_w, t_w) \approx F(\tau/t_w). \tag{5.4}$$

In Fig.(11) (Grenet and Delahaye, 2010) we show the low temperature ($T = 4K$) conductance, $G(V)$, of insulating granular aluminum thin films. A "three-step protocol" has been used in these experiments. After the sample is cooled with a gate voltage $V_g = V_{g1}$, a dip forms in $G(V)$ during a time t_{w1}, centered on the voltage V_{g1}. The gate voltage is then increased to V_{g2} for a time t_{w2}, and a new dip forms while the first one vanishes. The gate voltage is then changed to V_{g3}. The changing of the dip, ΔG_2, at V_{g2} is the measured quantity. ΔG_2 can be interpreted as the aging part of the conductance. The important thing to note is that ΔG_2 does depend on the aging times t_{w_1} and t_{w_2} and that there is t/t_{w_2} scaling. Again we emphasize that this simple aging phenomena is observed in numerous classical and quantum systems.

More complicated, or different, aging behavior is observed in disordered and strongly correlated metallic states. In fact, the change in the aging behavior from exotic to simple, has been related to the so-called metal-insulator transition in a two-dimensional electron system in MOSFETS that were fabricated on the (100) surface of Si. In this system the crucial quantity is the surface electron density, n_s. As n_s increases screening improves so that correlation effects become weaker, and at the same time the disorder is at least partly weakened since it is in part due to oxide charge scattering which is also better screened. The first crucial observations was that with decreasing density there is an apparent metal-insulator transition at $n_s = n_c$. Subsequent experiments (Bogdanovich and Popovic, 2002) on the metallic side showed an onset of glassy behavior at $n_s = n_g$ with $n_g > n_c$. This second observation showed there was an enormous increase in the low frequency noise for $n_s < n_g$, suggesting a sudden and dramatic slowing down of the electron dynamics. Later aging experiments were performed on the same system (Jarosznki and Popovic, 2007) .

The system was cooled to either $T = 0.5K$ or $T = 1.0K$ and an equilibrium conductivity $\sigma_o(n_s, T)$ was obtained with a gate voltage V_o. The gate voltage was then rapidly changed to a different value V_1, where it is kept for a time t_w. The voltage is then changed back to V_o, and the slowly evolving $\sigma(t, n_s, T)$ was measured. The results for $T = 1K$ are shown in Fig. (12). In the insulating phase, $n_s < n_c \simeq 4.5\pm0.4\times10^{11}cm^{-2}$, the systems exhibits simple aging with t/t_w scaling. In the metallic glassy region, $n_c < n_s < n_g \simeq 7.5\pm0.3\times10^{11}cm^{-2}$, there is aging with *exotic* scaling (Kurchan, 2002). That is, there is apparent t/t_w^{μ} scaling with μ an increasing function of n_s varying from $\mu = 1$, simple aging, at $n_s = n_c$ to $\mu \approx 3.5$ at $n_s = n_g$. This scaling with $\mu > 1$ is called super aging. Additional experiments probing DH in these systems would be most interesting.

Super or hyper aging behavior has also been observed in glassy liquids (Leheny and Nagel, 1998) and colloidal systems (nano-clay suspensions) (Shanin and Joshi, 2012). It also occurs in various random magnets and random field-like systems (Alberici-Kious *et al.*, 1998; Bouchaud *et al.*, 1997; Paul *et al.*, 2007). The connection between random field problems and RFOT is discussed in Section II.C.

B. Disordered and interacting electrons: Connections with random field problems and the glass transition problem

In Section II.C we considered the connection between random field magnetic problems and the SGT(Biroli *et al.*, 2013; Franz *et al.*, 2012, 2013). Here we discuss a connection between random field problems and the disordered and interacting electron problem (Belitz and Kirkpatrick, 1995a,b; Kirkpatrick and Belitz, 1995). Physically, since quenched disorder and electron-electron interactions in general frustrate one another, glassy behavior is anticipated.

Technically, the glassy nature of the interacting and disordered electron problem is also expected on general grounds. To see this we start with a schematic action for the problem:

$$S[\bar{\psi}, \psi] = S_o + S_{e-e} \tag{5.5}$$

where S_o is the noninteracting, disordered action,

$$S_o = -\sum_\sigma \int dx \bar{\psi}_\sigma(x) \left[\frac{\partial}{\partial \tau} - \frac{1}{2m}\nabla^2 - \mu + u(\mathbf{x}) \right] \psi_\sigma(x) \tag{5.6}$$

and S_{e-e} is the electron-electron interaction term:

$$S_{e-e} = \frac{\Gamma}{2} \int dx \bar{\psi}_{\sigma_1}(x) \bar{\psi}_{\sigma_2}(x) \psi_{\sigma_2}(x) \psi_{\sigma_1}(x) \tag{5.7}$$

Here $[\bar{\psi}, \psi]$ are fermion Grassmann fields, $x = (\mathbf{x}, \tau)$ with τ denoting imaginary time, $\int dx \equiv \int d\mathbf{x} \int_0^{1/T} d\tau$, m is the electron mass, μ is the chemical potential, σ is a spin label, and for simplicity we have assumed an instantaneous point-like electron-electron interaction with strength Γ. $u(\mathbf{x})$ is a random potential which represents the effects of disorder. We assume u to be δ-correlated, and obeys a Gaussian distribution with second moment

$$\{u(\mathbf{x})u(\mathbf{y})\} = \frac{1}{2\pi N_F \tau_{el}} \delta(\mathbf{x} - \mathbf{y}) \tag{5.8}$$

where the braces denote the disorder average. HereN_F is the (bare) density of states per spin at the Fermi surface and τ_{el} is the elastic mean free time.

Theories (Belitz and Kirkpatrick, 1994, 1997) for the MIT around its lower critical dimension indicate that the natural order parameter (OP) for the MIT is the single-particle density of states (DOS) at the Fermi surface, N. In terms of the Grassmann variables this quantity is $N = ImN(i\omega_n \to 0 + i0)$, with

$$N(i\omega_n) = N_n = -\frac{1}{2\pi N_F} \sum_\sigma < \bar{\psi}_{\sigma,n}(\mathbf{x}) \psi_{\sigma,\mathrm{n}}(\mathbf{x}) > \tag{5.9}$$

where we have normalized the DOS by $2N_F$. Equations (5.6) and (5.9) suggest that the OP for the MIT couples directly to the random potential u, and that this random field (RF) term is structurally identical to the one that appears in magnetic RF terms. Notice that this term is present in both interacting and noninteracting disordered electron problems, but in the interacting case there is an additional physical feature: The interaction term will in general favor a local electron arrangement that is different from the one favored by the random potential. This type of frustration is generally sufficient to lead to glassy behavior.

More formally, the theory using the replica trick to handle the disorder dependence and the replicated order parameter is (the spin dependence is suppressed for convenience)

$$Q^{\alpha\beta}_{nm}(\mathbf{x}) = \frac{1}{2}[\bar{\psi}^\alpha_n(\mathbf{x}) \psi^\beta_m(\mathbf{x}) + \bar{\psi}^\beta_m(\mathbf{x}) \psi^\alpha_n(\mathbf{x})] \tag{5.10}$$

with

$$< Q^{\alpha\beta}_{nm}(\mathbf{x}) >= \delta_{\alpha\beta}\delta_{nm} N_n \tag{5.11}$$

where now the angular brackets denote both a statistical mechanics average as well as a disorder average. The random field structure becomes apparent by transforming the field theory that is originally in terms of electron operators, to one in terms of the order parameter $Q^{\alpha\beta}$. Expanding that theory in deviation of Q from it's average value yields,

$$Q^{\alpha\beta}_{nm}(\mathbf{x}) =< Q^{\alpha\beta}_{nm}(\mathbf{x}) > + \phi^{\alpha\beta}_{nm}(\mathbf{x}) \tag{5.12}$$

The resulting theory has an expansion in powers of ϕ of the form,

$$S = S_2 + S_3 + S_4 + \cdots \tag{5.13}$$

with $S_j \sim \phi^j$. Explicitly,

$$S_2 = \int d\mathbf{x} tr \left[\phi(\mathbf{x}) \left(-\nabla^2 + m \right) \phi(\mathbf{x}) \right]$$

$$+ \frac{\Delta}{2} \int d\mathbf{x} \sum_{i=+,-} (tr_i \phi(\mathbf{x}))^2 \tag{5.14}$$

with m a mass-like term that is zero at zero frequency and at the metal-insulator transition (MIT) point where $N(0)$ is vanishes.

At Gaussian order the two point propagator for this theory in the replica limit is (Belitz and Kirkpatrick, 1995b; Kirkpatrick and Belitz, 1995),

$$< \phi_{12}(\mathbf{k}) \phi_{34}(-\mathbf{k}) >= \frac{-4\Delta\delta_{12}\delta_{34}\theta(n_1 n_3)}{(k^2 + m_{n_1 n_2})^2} + \cdots \tag{5.15}$$

where other terms in this correlation function involve only a single propagator and are therefore less singular. Here $1 = \alpha_1, n_1$ etc denotes replica and frequency. This correlation function is characteristic of a random field problem. Note that there are cubic terms in this theory, just as there are in the structural glass random field discussion of Section II.C.

So far an *epsilon*-expansion and ordinary and activated scaling theories of this approach to the MIT have been discussed. It is clear that many aspects of the RF strucure of the MIT need to be investigated. For example, is there a smeared dynamical glass transition quite apart from the MIT just as in the RFOT of the SGT transition? Is it related to the glassy behavior observed in the 2D MOSFETS that was discussed in Section V.A (see also, (Muller *et al.*, 2012))?

C. The metal-insulator transition and many-body localization

Apart from the 2D MOSFETS discussed in Section V.A, there has been an enormous amount of experimental work done on metal-insulator transitions in three-dimensional interacting and disordered electronic systems. The subject, however, remains controversial. Significant hysteresis effects are observed in $Ni(S, Se)_2$ and if conventional (as opposed to activated) scaling is assumed then the dynamical scaling exponent is surprisingly large (Husmann *et al.*, 1996). In the well studied

(Rosenbaum *et al.*, 1994; Stupp *et al.*, 1994) doped semiconductor SiP there are large sample to sample variations that are apparent only at very low temperatures, $T < 60mK$, suggesting equilibration problems due to very long relaxation times, and, possibly, dynamical heterogeneity effects. The glassy aspects of this has been discussed in detail elsewhere (Belitz and Kirkpatrick, 1995a). Related work on glassy features of MITs is considered in (Dobrosavljević *et al.*, 2012) .

More recently, other glassy aspects of the MIT and interacting and disordered electrons in general have become apparent. Following ideas of Anderson (Anderson, 1958) , Basko et. al (Basko *et al.*, 2006) suggested that it is possible for such a system to remain an insulator and nonergodic even at a non-zero temperature. Effectively, weakly interacting localized electrons cannot serve as their own heat bath, and consequently Mott's variable range hopping doesn't occur in the absence of delocalized phonons. The basic idea is that since the spectrum of localized electronic states is discrete the interaction between electrons will not in general have the *exact* energy difference to connect localized states and cause transport. This non-ergodic phase is called the many-body localized state. Basko et. al further argued that a system will remain an insulator and non-ergodic up to a critical temperature they denote by T_c and at $T > T_c$ the system will become ergodic and a metal. That is, the MIT occurs at finite temperature and is a sort of glass transition.

This idea has profound consequences not only for transport theory, but also for the foundations of quantum statistical mechanics. A basic tenant of statistical mechanics is that in a big system one can consider a smaller subsystem and the rest of the system acts as a heat bath for it. This apparently does not hold in a many-body localized phase.

There has been a a large amount of subsequent work on this problem (Bauer and Nayak, 2013; Huse and Oganesyan, 2013; Serbyn *et al.*, 2013). Bauer and Nayak theoretically and numerically investigated the entanglement entropy of excited states for a system of interacting and disordered one-dimensional spinless fermions. In the ground state the entanglement entropy $S(L)$ between a region of size L and the rest of the system satisfies an area law behaving for large L given by, [8],

$$S(L) = \alpha L^{d-1} + O(L^{d-2}) \tag{5.16}$$

where α is a constant. This is to be contrasted with highly excited or thermal states which in general satisfy a volume ($\sim L^d$) law. Importantly, Bauer and Nayak gave evidence that for many-body localized states the area law holds even for excited states as long as the interaction strength is not too large. In Fig. (13) we show numerical results for excited states for a quantity $a(L)$ that is closley related to the entropy. Here W is a measure of the disorder and V is a fermion interaction strength. The results indicate that for large disorder and small interactions the excited states obey an area entropy law and are thus many-body localized, but that for smaller disorder and larger interactions the entropy scale like a volume. This in turn is consistent with a finite temperature MIT and the considerations of (Basko *et al.*, 2006). Remarkably when this transition is approached from the metallic phase the results of (Bauer and Nayak, 2013) suggest there is a sort of Kauzmann or RFOT transition characterized by a vanishing entropy at a finite temperature.

[8] This is true for gapped systems. For gapless systems such as Fermi liquids there are logarithmic corrections.

D. Super glasses

In a very interesting paper Biroli, Chamon, and Zamponi (BCZ) (Biroli *et al.*, 2008; Nussinov, 2008) investigated the so-called super glass phase of matter which is simultaneously a superfluid and a frozen amorphous structure. Such a system can in principle be characterized experimentally by placing the system in a container rotating at a small frequency ω. If the system is a super solid, and if the frequency is not too high, than one would find the angular momentum of the solid is reduced from its classical value $I_{cl}\omega$ by a fraction f_s which is called the superfluid fraction.

BCZ employed a mapping between quantum Hamiltonians and classical Fokker-Planck operators, to a relate the ground state of a model of interacting Bosons to the Boltzmann measure of a classical hard sphere system. They further used this connection and known RFOT results for the glassy dynamics of Brownian hard spheres to work out the properties of the super glass phase and the quantum phase transition between the superfluid and super glass phases. In Fig. (3) we reproduce their phase diagram summarizing the mapping.

An important experimental question is if pure helium can form an amorphous phase. Simple monodisperse classical hard sphere systems quickly crystallize and the glassy phase can only be studied if the quenching rate is very fast. Superficially one expects the same behavior in helium. Indeed, path integral Monte Carlo simulations (Biroli *et al.*, 2011) of distinguishable He^4 rapidly quenched from the liquid phase to very much lower temperatures shows that the system crystallizes very quickly , without any sign of intermediate glassiness. Interestingly, it has been suggested that the neglected exchange interaction, and quantum fluctuations in general, can enhance glassiness.

This last point is very significant and can be understood using RFOT ideas (Foini *et al.*, 2010, 2011) [see also (Markland and et al., 2011; Zamponi, 2011)]. Consider a classical systems just above the ideal glass transition temperature with a configurational entropy $S_c(s)$ that is a function of the internal entropy s of the various mosaic states or clusters. The complexity is small, and in

general there will be more compact small entropy states than large s states. Now add a small amount of quantum fluctuations as measured by a hopping term $\sim J$. This hopping will not induce transitions into different mosaic states since that would involve the movement of a large number of particles which would be unlikely if J is small. Instead the quantum fluctuations will cause particle rearrangement within a given cluster. Now small cluster states cannot easily delocalize to lower their kinetic energy. Instead, adding the quantum fluctuations will favor larger entropy states that can more easily delocalize and get bigger. Since these states are less numerous, J has the effect of decreasing the complexity and can cause an ideal glass transition.

There is some experimental evidence for both super flow and glassiness in solid Helium at very low temperatures although the subject remains very controversial. Using a torsional oscillator experiment Rittner and Reppy (Reppy, 2010; Rittner and Reppy, 2007) observed a sample history dependence with large superfluid fractions ($\sim 20\%$) measured in quenched cooled samples that had small macroscopic dimensions, and saw reductions of the superfluid fraction that depended on how much the sample had annealed. This result would be consistent with a non-equilibrium glassy phase that was not stable. Ray and Hallock (Ray and Hallock, 2008, 2009) have performed experiments in which a chemical potential difference is applied across hcp solid helium at low densities by injecting liquid helium into one side of the solid. They observed a dc mass flow at temperatures below approximately 550mK. They also observed hysteresis effects: Samples thermally cycled to, or above, 550mK do not in general support flow when cooled down again. This memory effects is consistent with glassy-like behavior. More experiments are needed in these samples to see if flow is re-established at still lower temperatures. Still other experiments are needed to unambiguously confirm or otherwise the super glass phase of solid helium (Kim *et al.*, 2012; Mi *et al.*, 2014).

VI. SUMMARY AND DISCUSSION

All of the themes that we have highlighted in this article, which can be viewed from the perspective of concepts developed in glass physics, are active fields of research. It should be emphasized that our viewpoint is not universally endorsed, and hence there is a spirited debate on the origins of slow relaxation in glasses. It is unclear if there is an underlying structural order parameter describing the stability or dynamics glass forming systems. The search for such order parameter has been pursued for nearly thirty years, and it has been asserted that some sort of orientational order may increase upon supercooling. However, such a conclusion may only be relevant to quasi one component systems but the generality of this notion for complex glass forming materials is hardly obvious. In addition, the unambiguous demonstration of the existence of an the ideal glass transition temperature (T_K in the VFT fit) in experiments has been very difficult. For example, fitting viscosity data for Salol Fig.1a shows that temperatures at which reliable measurements can be made are far from T_K with $\epsilon \approx 0.26$ the dimensionless distance from the transition. It is even more difficult to show $T_K \neq 0$ in computer simulations although the plausibility of a thermodynamic transition envisioned in RFOT has been hinted at using random pinning simulations (Karmakar and Parisi, 2013; Kob and Berthier, 2013).

Despite these reservations in three key papers (Charbonneau *et al.*, 2013; Kurchan *et al.*, 2013, 2012)[see also (Kirkpatrick and Wolynes, 1987a)] , have studied in detail the thermodynamics of hard sphere particles in large dimensions ($d = \infty$) and all of the predictions of RFOT have been exactly demonstrated. By exploiting the observation that in this system at $d = \infty$ only the second virial coefficient contributes to the free energy functional of the system it was shown that the one step replica symmetry breaking (1RSB) and the two transitions (with the variable being density as opposed to temperature) scenario, as anticipated in the RFOT theory (Kirkpatrick and Thirumalai, 1989a), is valid. In addition, they discovered an instability of the 1RSB at high density resulting in the Gardner transition. It is generally believed that an inherently mean field description is reasonable for liquids (except close to gas-liquid critical point), and hence the large dimensional theory may have wider range of applicability (see, for example (Kirkpatrick, 1986; Marechal *et al.*, 2012).

We have barely touched on the potential application of glass transition concepts in biological problems. One noteworthy example is the folding of chromosomes, which could result in manifestation of metastability and glass-like behavior due to topological constraints (Hyeon and Thirumalai, 2011). In eukaryotic cells chromosomes fold into globules occupying well-defined regions referred to as chromosome territories (Cremer and Cremer, 2001), thus bringing widely separated gene-rich regions are brought into close proximity. Folding of chromosomes apparently occurs without forming knots, which is important for gene activity, in a polymer containing many mega base pairs. Using constraints derived from experiments as a guide (Lieberman-Aiden *et al.*, 2009) it has been argued that the genome is packaged into fractal globules (Grosberg *et al.*, 1993) differing qualitatively from equilibrium globules in which formation would occur with high probability. It is most likely the case that there are multiple states associated with fractal globules, which implies that the dynamics of chromosome folding would be glassy. Although the biological implications are unclear, it is worth exploring genome folding in various eukaryotic cells to assess if glass like behavior is exhibited, and to understand if nature utilizes such dynamics in of the most crucial functions.

There is an enormous amount of glassy phenomena that occur in the so-called hard condensed matter physics

systems. Generally these are quantum systems at low temperatures. They include Coulomb glasses, disordered insulators, disordered metals, quantum phase transitions from a superconducting state to either a disordered insulator or metal, various non-Fermi liquid systems, quantum Griffith's phase effects, etc. Even in low temperature ferromagnetic metals there are numerous manifestations of glassy effects (Kawasaki *et al.*, 2014). One of the main problems is that there is not a common language, let alone a common description, in these various subfields. It is possible that some of the recent unifying ideas in classical glassy systems will be relevant in these quantum systems. For example, in the SGT problem there has been a tremendous amount of work recently on dynamic heterogeneity. There has been a fruitful interplay between theory, simulations and experiments. This concept is also clearly relevant in biological glassy systems, as illustrated here. Recently, it has been shown that single molecule pulling experiments on proteins and DNA provide direct evidence for heterogeneity on the molecular scale (Hyeon *et al.*, 2014). In the condensed matter case this subject has hardly been touched (Nussinov *et al.*, 2013). In understanding the similarities and differences between classical and quantum glassiness two fundamental differences must be kept in mind. The first is that quenched disorder is perfectly correlated along the imaginary time direction and this can have especially profound implications for quantum phase transitions (Vojta, 2006). If the disorder is self-generated as in the case of the SGT, it is likely that similar profound effects will occur. The second is that in general there are modes that are soft only at $T = 0$, and these extra soft modes (Belitz and Kirkpatrick, 2014) will likely play an important role in the long time glassy dynamics.

Acknowledgments

We are grateful to Changbong Hyeon, Hongsuk Kang, Fracesco Zamponi, Stephen Kowalczykowski, Kingsuk Ghosh,Thierry Grenet, Dragana Popovic, and Chetan Nayak for providing us figures for reproduction. We thank Hongsuk Kang for useful discussions. We are grateful to the National Science Foundation for supporting this work through Grants No. CHE 13-61946 and No. DMR-09-01907.

References

Adam, G., and J. Gibbs (1965), J. Chem. Phys. **43**, 139.

Alberici-Kious, F., J. Bouchaud, L. Cugliandolo, P. Doussineau, and A. Levelut (1998), Phys. Rev. Lett. **81**, 4987.

Almendro, V., A. Marusyk, and K. Polyak (2013), Ann. Rev. Pathol. Med. Dis. **8**, 277.

Altschuler, S. J., and L. F. Wu (2010), Cell **141**, 559.

Amir, A., Y. Oreg, and Y. Imry (2011), Annual Review of Condensed Matter Physics **2**, 235.

Anderson, P. W. (1958), Phys Rev **109**, 1492.

Andreanov, A., G. Biroli, and J.-P. Bouchaud (2009), Europhys. Lett. **88**, 16001.

Anfinsen, C. B., and H. A. Scheraga (1975), Adv. Protein Chem. **29**, 205.

Angelini, T. E., E. Hannezo, X. Trepat, M. Marquez, J. J. Fredberg, and D. A. Weitz (2011), Proc. Natl. acad. Sci. **108**, 4714.

Barrat, J., J. Roux, and J. Hansen (1990), Chem. Phys. **149**, 197.

Baskakov, I., G. Legname, S. Prusiner, and F. Cohen (2001), J. Biol. Chem. **276**, 19687.

Basko, D. M., I. L. Aleiner, and B. L. Altshuler (2006), Ann of Phys **321**, 1126.

Bassler, H. (1987), Phys. Rev. Lett. **58**, 767.

Bauer, B., and C. Nayak (2013), J. of Stat. Mech: Theory and experiment , P09005.

Belitz, D., and T. R. Kirkpatrick (1994), Rev. Mod. Phys. **66**, 261.

Belitz, D., and T. R. Kirkpatrick (1995a), Phys Rev B **52**, 13922.

Belitz, D., and T. R. Kirkpatrick (1995b), Z. Phys B **98**, 513.

Belitz, D., and T. R. Kirkpatrick (1997), Phys. Rev. B **56**, 6513.

Belitz, D., and T. R. Kirkpatrick (2014), Phys. Rev. B **89**, 035130.

Bengtzelius, U., W. Goetze, and A. Sjolander (1984), J. Phys. C **17**, 5915.

Berthier, L. (2011), Physics **4**, 42.

Berthier, L., and G. Biroli (2011), Rev. Mod. Phys. **83**, 587.

Berthier, L., and W. Kob (2012), Phys. Rev. E. **85**, 011102.

Binder, K., and A. Young (1986), Rev. Mod. Phys. **58**, 801.

Biroli, G., and J. P. Bouchaud (2012), in *Structural glasses and supercooled liquids: theory, experiment and applications*, edited by V. Lubchenko and P. Wolynes (Johh-Wiley) pp. 31–114.

Biroli, G., J. P. Bouchaud, A. Cavagna, T. S. Grigera, and P. Verrocchio (2008), Nat. Phys. PHYSICS **4**, 771.

Biroli, G., B. Clark, L. Foini, and F. Zamponi (2011), Phys Rev B **83**, 09450.

Biroli, G., and J. P. Garrahan (2013), J. Chem. Phys. **138**.

Biroli, G., S. Karmakar, and I. Procaccia (2013), Phys. Rev. Lett. **111**, 165701.

Bogdanovich, S., and D. Popovic (2002), Phys Rev. Lett **88**, 236401.

Borman, S. (2010), Chem. Eng. News. **88**, 36.

Bouchaud, J., and G. Biroli (2004), J. Chem. Phys. **121**, 7347.

Bouchaud, J., and G. Biroli (2005), Phys. Rev. B. **72**, 064204.

Bouchaud, J.-P., L. F. Cugliandolo, J. Kurchan, and M. Mezard (1997), in *Spin glasses and random fields*, edited by A. Young (World Scientific) pp. 161–224.

Bryngelson, J. D., and P. G. Wolynes (1989), J. Phys. Chem. **93**, 6902.

CA, C. A., M. DR, and O. M (1986), Ann. NY. Acad. Sci. **484**, 241.

Camacho, C., and D. Thirumalai (1993a), Proc. Natl. Acad. Sci. **90**, 6369.

Camacho, C. J., and D. Thirumalai (1993b), Phys. Rev. Lett. **71** (15), 2505.

Charbonneau, P., J. Kurchan, G. Parisi, P. Urbani, and F. Zamponi (2013), arXiv: 1310.2549 .

Chothia, C. (1992), Nature **357**, 543.

Cohen, A. A., N. Geva-Zatorsky, E. Eden, M. Frenkel-Morgenstern, I. Issaeva, A. Sigal, R. Milo, C. Cohen-Saidon, Y. Liron, Z. Kam, L. Cohen, T. Danon, N. Perzov, and U. Alon (2008), Science **322**, 1511.

Cremer, T., and C. Cremer (2001), Nature Rev. Genet. **2** (4), 292.

Cummins, H. (1999), J. Phys. Cond. **11**, A95.

Dasgupta, C., A. Indrani, S. Ramaswamy, and M. Phani (1991), Europhys. Lett. **15**, 307.

Dasgupta, C., and O. Valls (1999), Phys. Rev. E. **59**, 3123.

Dauchot, O., and E. Bertin (2012), Phys. Rev. E **86**, 036312.

Dauchot, O., and E. Bertin (2013), arXiv: 1310.6967 , XXX.

Derrida, B. (1981), Phys. Rev. B **24**, 2613.

Dill, K. A., S. B. Ozkan, M. S. Shell, and T. R. Weikl (2008), Annu. Rev. Biophys. **37**, 289.

Ditzler, M. A., D. Rueda, J. Mo, K. Hakansson, and N. G. Walter (2008), Nucleic Acis Res. **36** (22), 7088.

Dobrosavljević, V., N. Trivedi, and J. M. V. jr, Eds. (2012), *Conductor insulator quantum phase transitions* (Oxford University Press, Oxford).

Donati, C., S. Franz, S. C. Glotzer, and G. Parisi (2002), J. Non-Cryst. Solids **307**, 215.

Dyre, J. (1998), J. Non-Cryst. Sol. **235**, 142.

Ediger, M. (2000), Ann. Rev. Phys. Chem. **51**, 99.

Ediger, M. D., and P. Harrowell (2012), J. Chem. Phys. **137**, 080901.

Edwards, S., and P. Anderson (1975), J. Phys. F. **5**, 965.

Fisher, D., and D. Huse (1988), Phys. Rev. B **38**, 373.

Fisher, M., and A. Berker (1982), Phys. Rev. B **26** (5), 2507.

Foini, L., G. Semerjian, and F. Zamponi (2010), Phys Rev Lett **105**, 167204.

Foini, L., G. Semerjian, and F. Zamponi (2011), Phys Rev B **83**, 094530.

Franz, S., H. Jacquin, G. Parisi, P. Urbani, and F. Zamponi (2012), PNAS **109**, 18725.

Franz, S., G. Parisi, F. Ricci-Tersenghi, and T. Rizzo (2013), J. Stat. Phys. , L02001.

Frauenfelder, H., F. Parak, and R. Young (1988), Annu. Rev. Biophys. Biophys. Chem. **17** (1), 451.

Garrahan, J. P. (2011), Proc. Natl. Acad. Sci. **108**, 4701.

Goetze, W. (2009), *Complex Dynamics of glass forming liquids. A mode-coupling theory* (Oxford University Press).

Goldstein, M. (1969), J. Chem. Phys. **51**, 3728.

Grenet, T., and J. Delahaye (2010), Eur Phys Journal B **76**, 229.

Grosberg, A., Y. Rabin, S. Havlin, and A. Neer (1993), Europhys. Lett. **23**, 373.

Gross, D. J., and M. Mezard (1984), Nuc. Phys. B **240**, 431.

Heppner, G., and B. Miller (1983), Cancer and Metastasis Reviews **2**, 5.

Herms, A., M. Bosch, N. Ariotti, B. J. N. Reddy, A. Fajardo, A. Fernandez-Vidal, A. Alvarez-Guaita, M. A. Fernandez-Rojo, C. Rentero, F. Tebar, C. Enrich, M.-I. Geli, R. G.

Parton, S. P. Gross, and A. Pol (2013), Curr. Biol **23**, 1489.
Hofmann, H., A. Soranno, A. Borgia, K. Gast, D. Nettels, and B. Schuler (2012), Proc. Natl. acad. Sci. **109**, 16155.
Huse, D., and D. Fisher (1987), J. Phys. A. **20**, L997.
Huse, D. A., and V. Oganesyan (2013), arXiv:1305.4915 .
Husmann, A., D. Jin, Y. Zastarker, T. Rosenbaum, X. Yao, and J. Honig (1996), Science **274**, 1874.
Hyeon, C., M. Hinczewski, and D. Thirumalai (2014), Phys. Rev. Lett. **112**, 138101.
Hyeon, C., J. Lee, J. Yoon, S. Hohng, and D. Thirumalai (2012), Nat. Chem. **4**, 907.
Hyeon, C., and D. Thirumalai (2011), Nat. Commun. **2:487**, 10.1038/ncomms1481.
Ikeda, A., and K. Miyazaki (2010), Phys Rev Lett **104**, 255704.
Jarosznki, J., and D. Popovic (2007), Phys Rev Lett **99**, 216401.
Kang, H., T. R. Kirkpatrick, and D. Thirumalai (2013), Phys. Rev. E. **88**, 042308.
Karmakar, S., C. Dasgupta, and S. Sastry (2009), Proc. Natl. acad. Sci. **106**, 3675.
Karmakar, S., and G. Parisi (2013), Proc. Natl. Acad. Sci. **110**, 2752.
Kauzmann, W. (1948), Chem. Rev. , 219.
Kawasaki, I., M. Yokoyama, S. Nakano, K. Fujimura, N. Netsu, H. Kawanaka, and K. Tenya (2014), J. Phys. Soc. Jpn. **83**, 064712.
Kim, D. Y., J. T. West, T. A. Engstrom, N. Mulders, and M. H. W. Chan (2012), Phys. Rev. B **85**, 024533.
Kim, E., and M. Chan (2004), Nature **427**, 275.
Kim, K., and S. Saito (2013), J. Chem. Phys. **138**, 12A506.
Kirkpatrick, T., and D. Thirumalai (1989a), J. Phys. A. **22**, L149.
Kirkpatrick, T., and D. Thirumalai (2014), arXiv.org , 1401.2024.
Kirkpatrick, T. R. (1986), J. Chem. Phys. **85**, 3515.
Kirkpatrick, T. R., and D. Belitz (1995), Phys Rev. Lett **74**, 1178.
Kirkpatrick, T. R., and D. Thirumalai (1987a), Phys. Rev. Lett. **58**, 2091.
Kirkpatrick, T. R., and D. Thirumalai (1987b), Phys. Rev. B **36**, 5388.
Kirkpatrick, T. R., and D. Thirumalai (1988a), Phys. Rev. A **37**, 4439.
Kirkpatrick, T. R., and D. Thirumalai (1988b), Phys. Rev. B **37**, 5342.
Kirkpatrick, T. R., and D. Thirumalai (1989b), J. Phys. A **22**, L149.
Kirkpatrick, T. R., and D. Thirumalai (1995a), Transp. Theor. and Stat. Phys. **24**, 927.
Kirkpatrick, T. R., and D. Thirumalai (1995b), J. de Physique I **5**, 777.
Kirkpatrick, T. R., D. Thirumalai, and P. G. Wolynes (1989), Phys. Rev. A **40**, 1045.
Kirkpatrick, T. R., and P. G. Wolynes (1987a), Phys. Rev. A **35**, 3072.
Kirkpatrick, T. R., and P. G. Wolynes (1987b), Phys. Rev. B. **36**, 8552.
Kob, W., and L. Berthier (2013), Phys. Rev. Lett. **110**, 245702.
Kurchan, J. (2002), Phys. Rev. E. **66**, 01710.
Kurchan, J., G. Parisi, P. Urbani, and F. Zamponi (2013), J. Phys. Chem. B **117**, 12979.
Kurchan, J., G. Parisi, and F. Zamponi (2012), J. Stat. Phys. , P10012.
Leheny, R., and S. Nagel (1998), Phys. Rev. B **57**, 5154.
Leutheusser, E. (1984), Phys. Rev. A. **29** (5), 2765.
Li, H., N. Winfreen, and C. Tang (1996), Science **273** (5275), 666.
Lieberman-Aiden, E., N. van Berkum, L. Williams, M. Imakaev, T. Ragoczy, A. Telling, I. Amit, B. Lajoie, P. Sabo, M. Dorschner, *et al.* (2009), Science **326** (5950), 289.
Lin, M. M., and A. H. Zewail (2012), Proc. Natl. Acad. Sci. **109**, 9851.
Lindsay, H. M., and P. M. Chaikin (1982), J. Chem. Phys. **76**, 3774.
Liu, B., R. J. Baskin, and S. C. Kowalczykowski (2013), Nature **500**, 482.
Lubchenko, V., and P. G. Wolynes (2007), Ann. Rev. Phys. Chem. **58**, 235.
Lushnikov, A. Y., A. Bogdanov, and Y. L. Lyubchenko (2003), J. Biol. Chem. **278** (44), 43130.
Marechal, M., U. Zimmermann, and H. Lowen (2012), J. Chem. Phys. **136**, 144506.
Markland, T. E., and et al. (2011), Nature Physics **7**, 134.
Mezard, M. (1987), *Spin Glass Theory and Beyond*, Lecture Notes in Physics, Vol. 9 (World Scientific).
Mezard, M., and G. Parisi (1996), J. Phys. A **29**, 6515.
Mi, X., A. Eyal, A. Talanov, and J. Reppy (2014), arXiv , 1407.1515.
Moore, M., and B. Drossel (2002), Phys. Rev. Lett. **89**, 217202.
Mountain, R. D., and D. Thirumalai (1987), Phys. Rev. A **36**, 3300.
Muller, M., P. Strack, and S. Sachdev (2012), Phys. Rev. A **86**, 023604.
Nattermann, T. (1997), in *Spin glasses and random fields*, Series on directions in condensed matter physics, Vol. 12, edited by A. Young (World Scientific).
Novikov, V., and A. Sokolov (2003), Phys. Rev. E **67**, 031507.
Nussinov, Z. (2008), Physics **1**, 40.
Nussinov, Z., P. Johnson, M. J. Graf, and A. V. Balatsky (2013), Phys. Rev. B **87**, 184202.
Okumus, B., T. J. Wilson, D. M. J. Lilley, and T. Ha (2004), Biophys. J. **87**, 2798.
Onuchic, J., Z. Luthey-Schulten, and P. G. Wolynes (1997), Ann. Rev. Phys. Chem. **48**, 539.
Ovadyaha, Z. (2006), Phys Rev B **73**, 214204.
Palmer, R. (1982), Adv. Phys. **31**, 669.
Pan, J., D. Thirumalai, and S. A. Woodson (1997), J. Mol. Biol. **273** (1), 7.
Parisi, G., and F. Zamponi (2010), Rev. Mod. Phys. **82**, 789.
Paul, R., G. Schehr, and H. Rieger (2007), Phys Rev E **75**, 030104(R).
Pelkmans, L. (2012), Science **336**, 425.
Pollack, M., and M. Ortuno (1985), in *Electron electron interactions in disordered systems*, Modern problems in condensed matter science, Vol. 10, edited by A. L. Efros and M. Pollack (Elsevier Science) p. 287.
Pollack, M., M. Ortuno, and A. Frydman (2013), *The electron glass* (Cambride University Press).
Ramakrishnan, T., and M. Yussouff (1979), Phys. Rev. B **19**, 2775.
Ray, M. W., and R. B. Hallock (2008), Phys Rev Lett **100**, 235301.
Ray, M. W., and R. B. Hallock (2009), Phys Rev B **79**,

224302.
Reppy, J. D. (2010), Phys Rev Lett **104**, 255301.
Rittner, A. S. C., and J. D. Reppy (2007), Phys Rev Lett **98**, 175302.
Rosenbaum, T. F., G. A. Thomas, and M. A. Paalanen (1994), Phys Rev Lett **72**, 2121.
Sato, T., F. Kagawa, K. Kobayashi, K. Miyagawa, K. Kanoda, R. Kumai, Y. Murakami, and Y. Tokura (2014), Phys. Rev. B **89**, 121102.
Schmalian, J., and P. G. Wolynes (2000), Phys Rev Lett **85**, 836.
Schmid, B., and R. Schilling (2010), Phys. Rev. E **81**, 041502.
Schuler, B., and W. A. Eaton (2008), Curr. Opin. Struct. Biol. **18**, 16.
Schultes, E. A., and D. P. Bartel (2000), Science **289**, 448.
Serbyn, M., Z. Papic, and D. Abanin (2013), Phys Rev Lett **110**, 260601.
Shakhnovich, E. (2006), Chem. Rev. **106**, 1559.
Shanin, A., and Y. Joshi (2012), Langmuir **28**, 5826.
Shi, Z., P. G. Debenedetti, and F. H. Stillinger (2013), J. Chem. Phys. **138**.
Sillescu, H. (1999), J. Non-Cryst. Solids **243**, 81.
Sillescu, H., R. Bohmer, G. Diezemann, and G. Hinze (2002), J. Non-Cryst. Solids **307**, 16.
Singh, Y., J. Stoessel, and P. Wolynes (1985), Phys. Rev. Lett. **54**, 1059.
Socci, N. D., and J. N. Onuchic (1995), J. Chem. Phys. **103** (11), 4732.
Solomatin, S. V., M. Greenfeld, S. Chu, and D. Herschlag (2010), Nature **463**, 681.
Spencer, S. L., S. Gaudet, J. G. Albeck, J. M. Burke, and P. K. Sorger (2009), Nature **459**, 428.
Struik, L. C. E. (1977), *Physical aging in plastics and other glassy materials* (Elsevier Scientific Publishing).
Stryer, L. (1988), *Biochemistry* (W.H. Freeman).
Stupp, H., M. Hornung, M. Lakner, O. Madel, and H. v. Lohneysen (1994), Phys Rev Lett **72**, 2122.
Sturn, A., J. Quackenbush, and Z. Trajanoski (2002), Bioinformatics **18** (1), 207.
Szamel, G., and E. Flenner (2011), Phys. Rev. Lett. **107**, 105505.
Takada, S., J. Portman, and P. Wolynes (1997), Proc. Natl. Acad. Sci. **94**, 2318.
Tamayo, P., D. Slonim, J. Mesirov, Q. Zhu, S. Kitareewan, E. Dmitrovsky, E. S. Lander, and T. R. Golub (1999), Proc. Natl. Acad. Sci. USA **96**, 2907.
Thirumalai, D. (1995), J. Phys. I (Fr.) **5**, 1457.
Thirumalai, D., V. Ashwin, and J. Bhattacharjee (1996), Phys. Rev. Lett. **77**, 5385.
Thirumalai, D., and C. Hyeon (2005), Biochemistry **44** (13), 4957.
Thirumalai, D., and T. R. Kirkpatrick (1988), Phys. Rev. B **38**, 4881.
Thirumalai, D., D. Klimov, and R. Dima (2003), Curr. Opin. Struct. Biol. **13**, 146.
Thirumalai, D., and D. K. Klimov (1999), "Stochastic dynamics and pattern formation in biological and complex systems," Chap. Emergence of stable and fast folding structures (American Institute of Physics) pp. 96–111.
Thirumalai, D., N. Lee, S. A. Woodson, and D. K. Klimov (2001), Annu. Rev. Phys. Chem. **52**, 751.
Thirumalai, D., and R. D. Mountain (1993), Phys. Rev. E **47**, 479.
Thirumalai, D., R. D. Mountain, and T. R. Kirkpatrick (1989a), Phys. Rev. A **39**, 3563.
Thirumalai, D., R. D. Mountain, and T. R. Kirkpatrick (1989b), Phys. Rev. A. **39**, 3563.
Thirumalai, D., E. P. O'Brien, G. Morrison, and C. Hyeon (2010), Annu. Rev. Biophys. **39**, 159.
Toninelli, C., M. Wyart, L. Berthier, G. Biroli, and J.-P. Bouchaud (2005), Phys. Rev. E **71**, 041505.
Villain, J. (1985), J. de. Physique **46** (11), 1843.
Vojta, T. (2006), J. Phys. A **39**, R143.
Young, A. P., Ed. (1998), *Spin glasses and random fields*, Direction in condensed matter physics, Vol. 12 (World Scientific).
Zamponi, F. (2011), Nature Physics **7**, 99.
Zhuang, X., H. Kim, M. Pereira, H. Babcock, N. Walter, and S. Chu (2002), Science **296**, 1473.
Zwanzig, R. (1988), Proc. Natl. Acad. Sci. USA **85**, 2029.

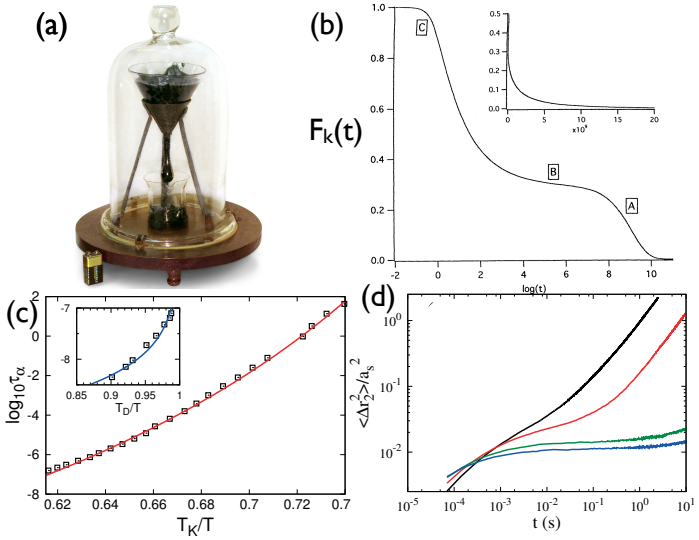

Figure 1 General characteristic of glassy systems. (a) Dramatic illustration of flow of highly viscous material bitumen in an hour glass. The experiment was initiated in in 1927 and to date only about nine drops have fallen. The viscosity of bitumen is about 230 billion times that of water. (b) Decay of the intermediate scattering function versus $\log(t)$ is schematically displayed for a slightly undercooled liquid. The long time α-relaxation time is given by regime A and the short time decay corresponds to regime C. In the intermediate B regime there is a typically two-step relaxation, which is in accord with the Mode Coupling Theory. The same plot is displayed in the inset as a function of t, which shows only the long time decay. The figure is adopted from (Cummins, 1999). (c) Dependence of the α-relaxation time, τ_α, (regime A in (b)) for salol as a function of T_K/T with the fit given by Eq. 1.1. The inset shows τ_α as a function of T_D/T where T_D is the dynamical transition temperature. (d) Dependence of the mean square displacement of a particle as a function of time, t, at various volume fractions for a binary mixture of charge colloidal suspension, which forms a Wigner glass.

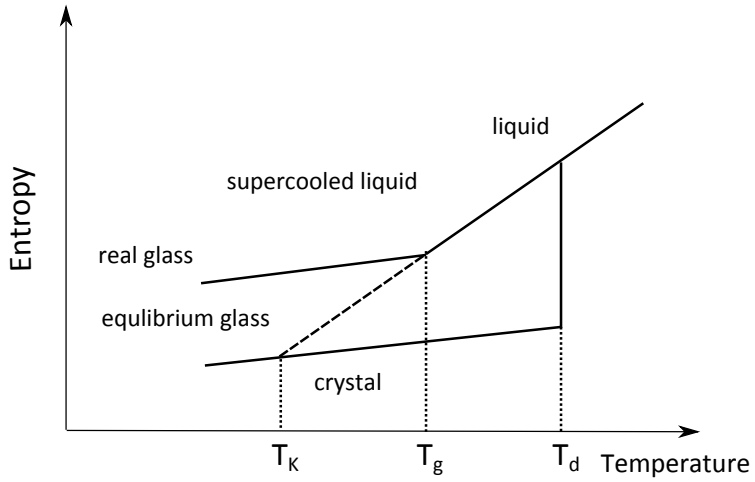

Figure 2 Schematic representation of the configurational entropy change as the temperature of a liquid is reduced. Below the temperature T_d, which is an avoided dynamical transition, transport occurs by crossing free energy barriers. At $T < T_g$, the glass temperature, the supercooled liquid falls out of equilibrium. However, if the entropy of the supercooled liquid is extrapolated (dashed line) it would equal the value of the crystal at T_K, the Kauzmann temperature.

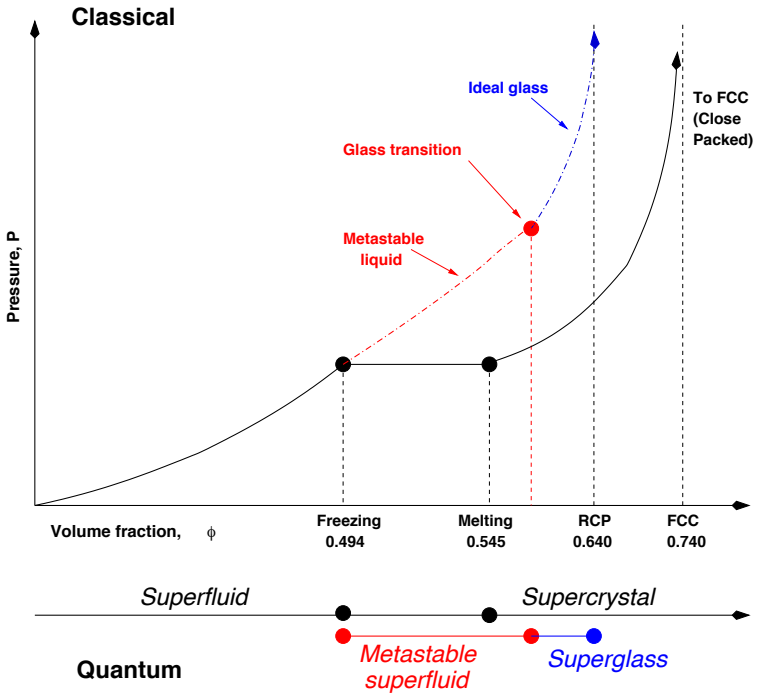

Figure 3 Diagram of states for a classical and quantum hard sphere fluids. The top panel shows the expected phases as the volume fraction is increased. Transitions to metastable liquid and glassy phases are in red. The expected transition to an ideal glassy state, predicted to occur at ϕ close to the random close packing (RCP) is shown in blue. The lines at the bottom show onset of distinct phases when quantum effects are taken into account. These are further discussed in Section V.

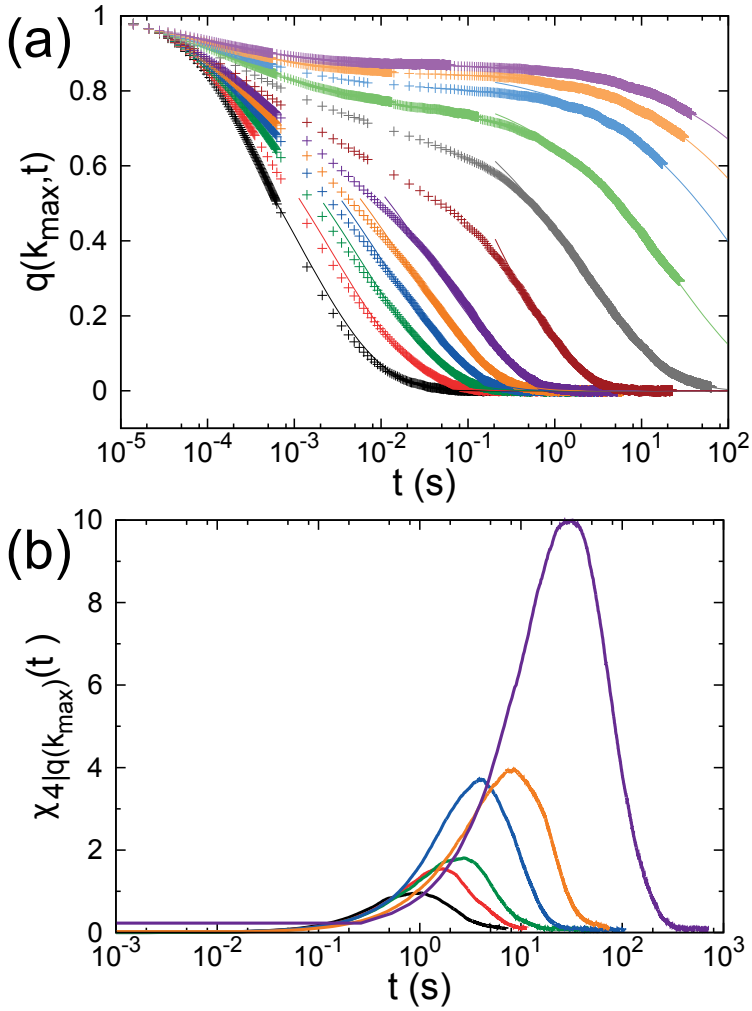

Figure 4 (a) Scattering function for a binary mixture of charged colloidal suspensions calculated from Brownian dynamics simulations. The mixture consists of equal number of large and small highly charged spherical particles. We show $q(k_{max}, t)$ for the small particles at k_{max} corresponding to the inverse of the location corresponding to the first maximum in the pair function. The volume fraction increases from top to bottom as 0.01, 0.02, 0.03, 0.04, 0.05, 0.06, 0.075, 0.1, 0.125, 0.15, 0.175, and 0.2. The lines are fits to $q(k_{max}, t) = exp - (t/\tau_\alpha)^\beta$ with ϕ-independent $\beta = 0.45$. (b) Time-dependent changes in the four point susceptibility, showing fluctuations in $q(k_{max}, t)$ for $\phi = 0.02$, 0.03, 0.04, 0.05, 0.06, and 0.075 from left to right. These figures are adapted from (Kang *et al.*, 2013).

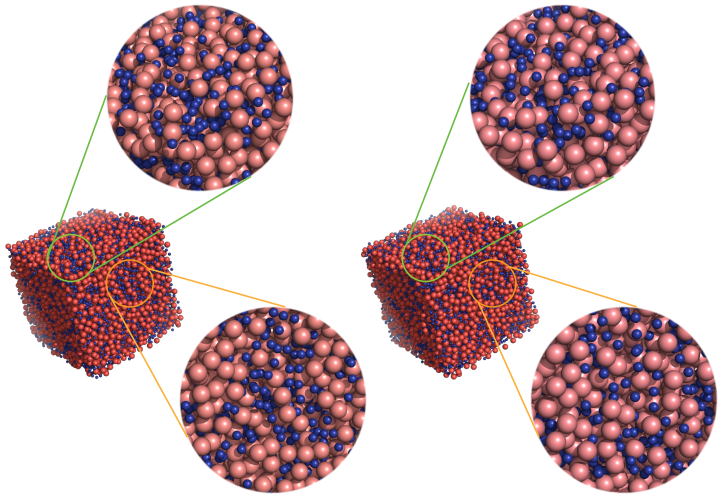

Figure 5 Schematic illustration of dynamic heterogeneity in three dimensional binary mixture of charged colloidal suspensions. The three figures on the left show a sample prepared at a given time, t, for $\phi = 0.10$, which is close to ϕ_d. The snapshot for two subsamples are shown above and below. The three figures on the right are the same snapshots at a later time $t' \approx t + \tau_\alpha$. The subsamples on the top are essentially identical where as the ones at the bottom are quite different. Even though there are a large number of particles within each subsample their time evolutions are very different indicating considerable subsample-to-subsample variations. This observation leading to violation of law of large numbers and loss in ergodicity is indicative of dynamical heterogeneity. These schematic illustrations affirms the mosaic picture of glassy states and shows that only by following the subsamples as a function of time can the extent of dynamic heterogeneity be assessed.

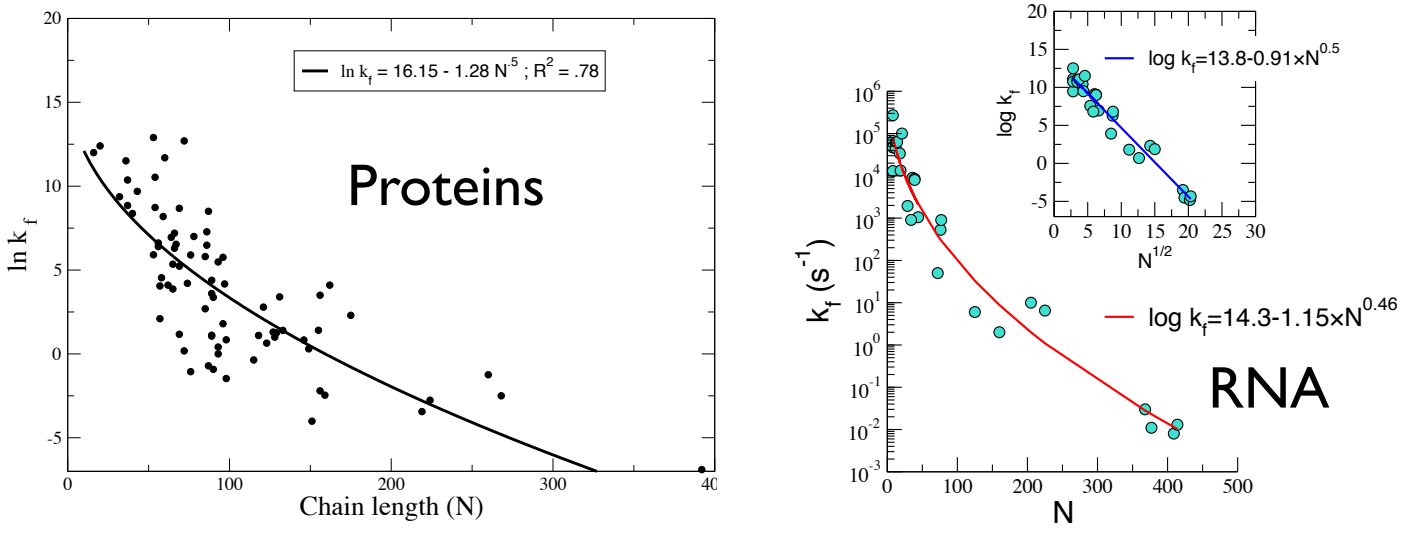

Figure 6 Dependence of the folding rates of proteins (left) and RNA (right) as a function of length. The fits are based on predictions using $k_F \approx e^{\sqrt{(N)}}$, which follows from activated scaling ideas described in Section IID.

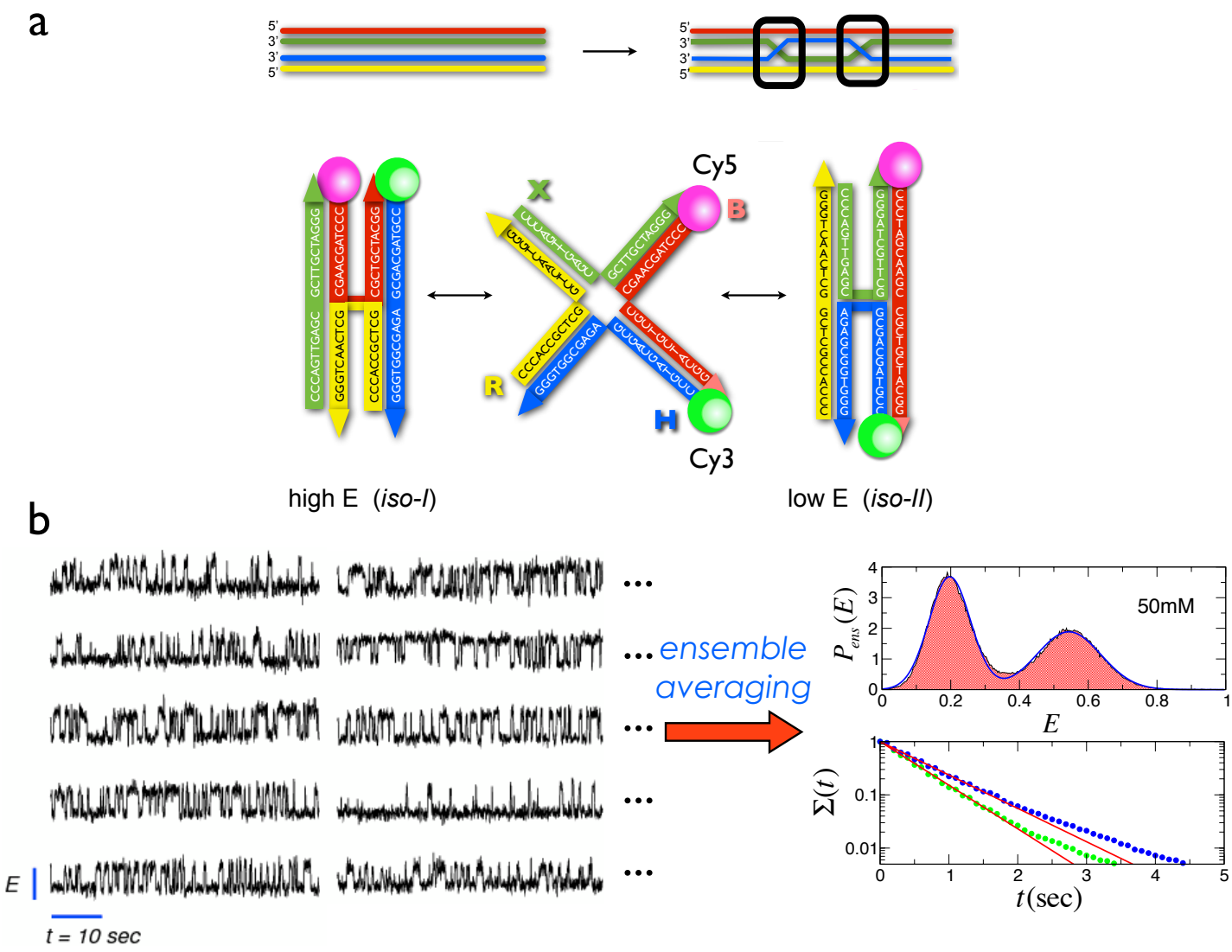

Figure 7 HJ dynamics probed using smFRET experiments. **a.** Strand exchange in DNA recombination (top) and the two isoforms of the Holliday Junction connected by the open square structure (bottom). The Cy5 (magenta) and Cy3 (green) dyes, attached to the B and H branches in smFRET experiments, are represented as spheres. **b.** FRET time traces ($\{E_i(t)\}$ with $i = 1, 2, \ldots, N$ with $N = 315$) obtained for individual HJ molecules at $[Mg^{2+}] = 50$ mM. The ensemble averaged histogram of the FRET efficiency E, i.e., $P_{ens}(E)$, fits to a double-Gaussian curve (blue line), and the dwell time distribution (bottom panel) for low (data in green) and high (data in blue) FRET states are approximately fit to single exponential functions (red lines).

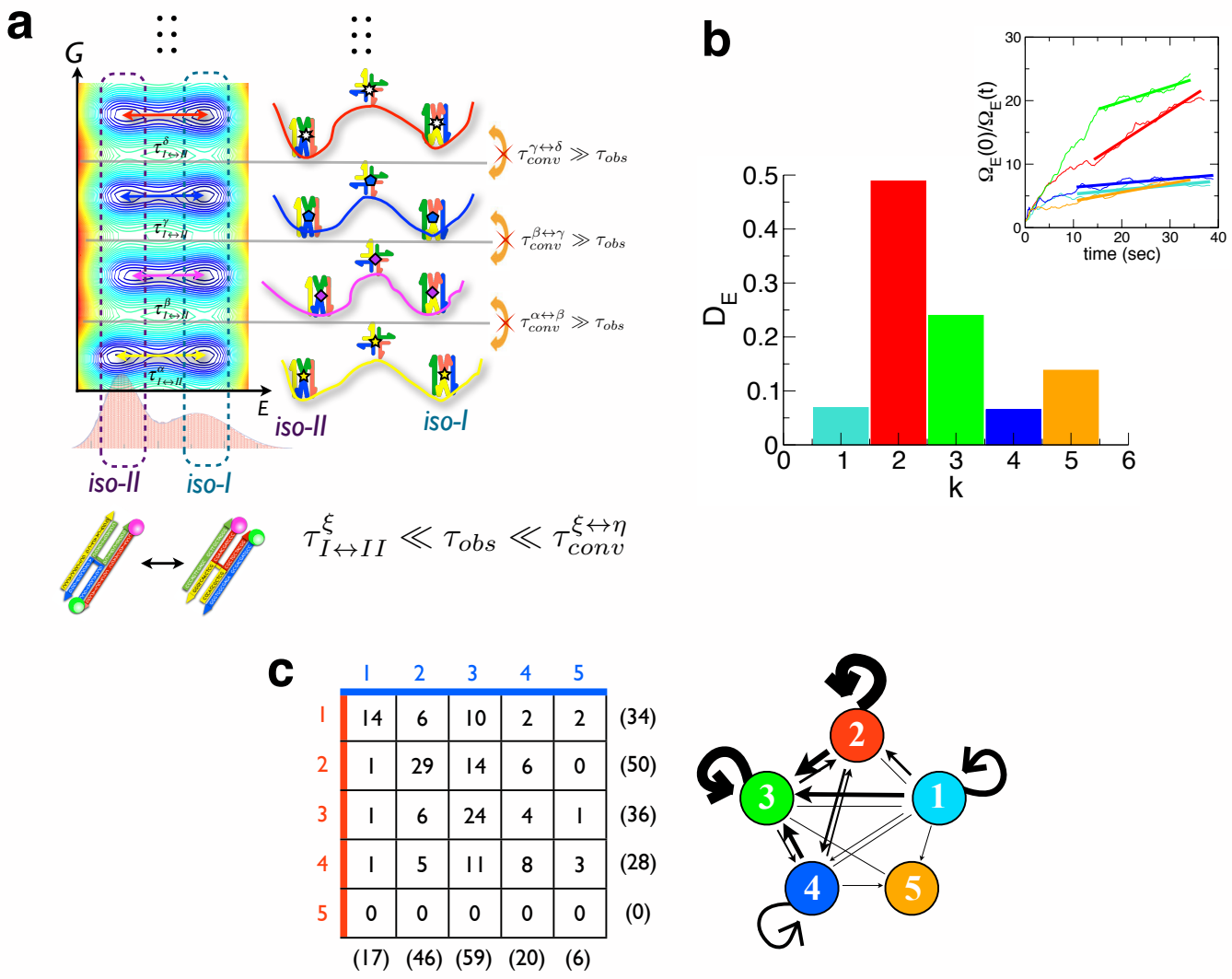

Figure 8 **a.** Model for the dynamics of HJ constructed based on experiments and simulations reported in (Hyeon *et al.*, 2012). The free energy contours for various states are on the left. The isoforms (Fig. 7a) in each state are connected open square form. Ensemble averaged distribution of the FRET efficiencies, $P_{ens}(E)$, is shown at the bottom. On the right schematic of the free energy profiles are shown with the cartoons of HJ structures. The symbols (star, pentagon, ...) at the junction emphasize that the junction structure is intact during the isomerization process. Consequently, $\tau^{\xi}_{\mathrm{I}\leftrightarrow\mathrm{II}}$ ($\xi = \alpha, \beta \ldots$) $\ll \mathcal{T}_{obs} \ll \tau^{\xi\leftrightarrow\eta}_{conv}$ ($\xi, \eta = \alpha, \beta, \gamma, \ldots$ with $\xi \neq \eta$) is established. **b.** Five ergodic components are needed to partition the set of stationary distributions of FRET efficiencies is five. The rates, D_Es, of exploration of the conformational space obtained from the ergodic measure, $\Omega_E(t) = \frac{1}{N}\sum_{i=1}^{N}\left(\varepsilon_i(t) - \overline{\varepsilon(t)}\right)^2$ with $\overline{\varepsilon(t)} \equiv \frac{1}{N}\sum_{i=1}^{N}\varepsilon_i(t)$ (shown on top), are different in the distinct ergodic components. Here, $\varepsilon_i(t)$ is the running time average of the FRET efficiency for molecule i, which can be caculated using trajectories in Fig. 7b. **c.** Evidence for interconversion between ergodic components by Mg^{2+} reset experiments in 148 molecules. The indices at the sides of matrix and in the nodes denote the cluster number $k = 1, 2 \ldots 5$. The numbers in the parentheses are the occupation number in each cluster, which can be obtained by summing up the transition frequency from one cluster to the other. The diagram on the right is the kinetic network describing the HJ transition under Mg^{2+} pulse. The widths of the arrows are proportional to the number of transitions.

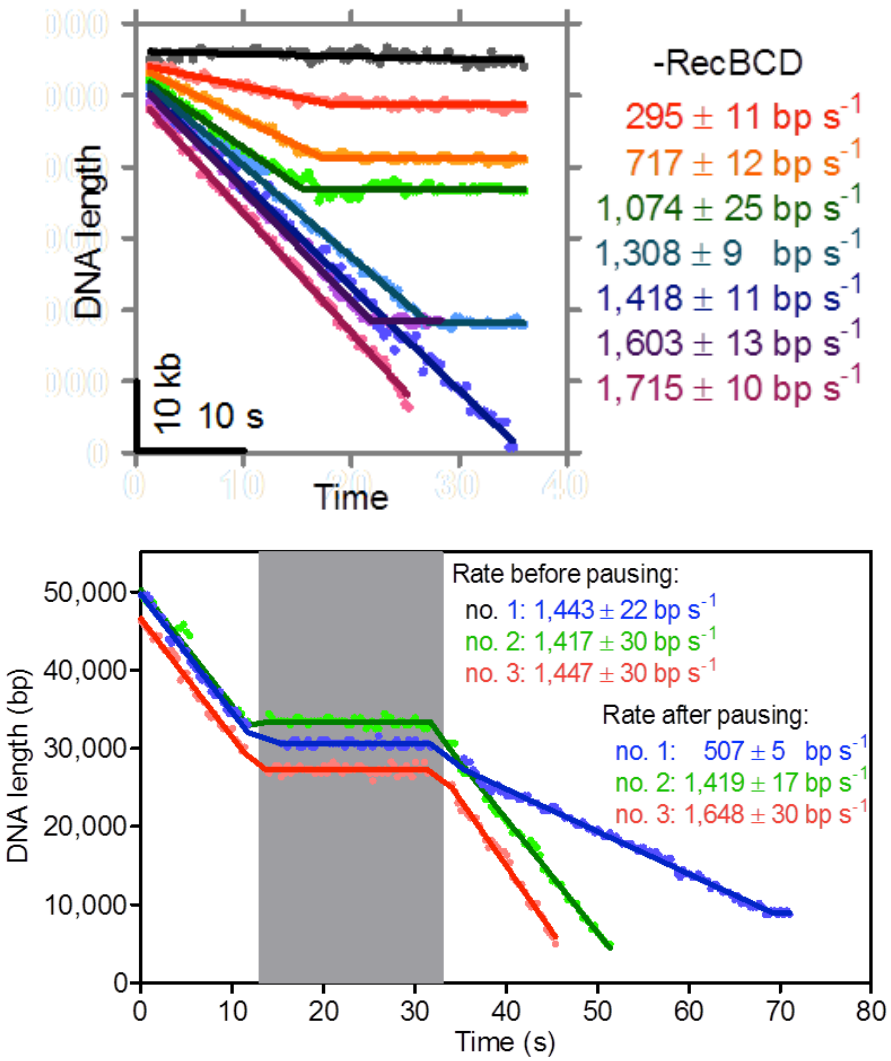

Figure 9 Top panel gives the lenghth of DNA unwound of various RecBCD motors for various molecules. Black line is for a system without RecBCD. The unwinding velocities, listed on the right, varies greatly depending on the molecule. Bottom panel gives the result of reset experiment in which the motor is depleted of the ligand for a period of time and reintroduced to resume unwinding. The velocities of the three motors vary greatly after reset and suggests that the function before and after reset probe distinct ergodic components.

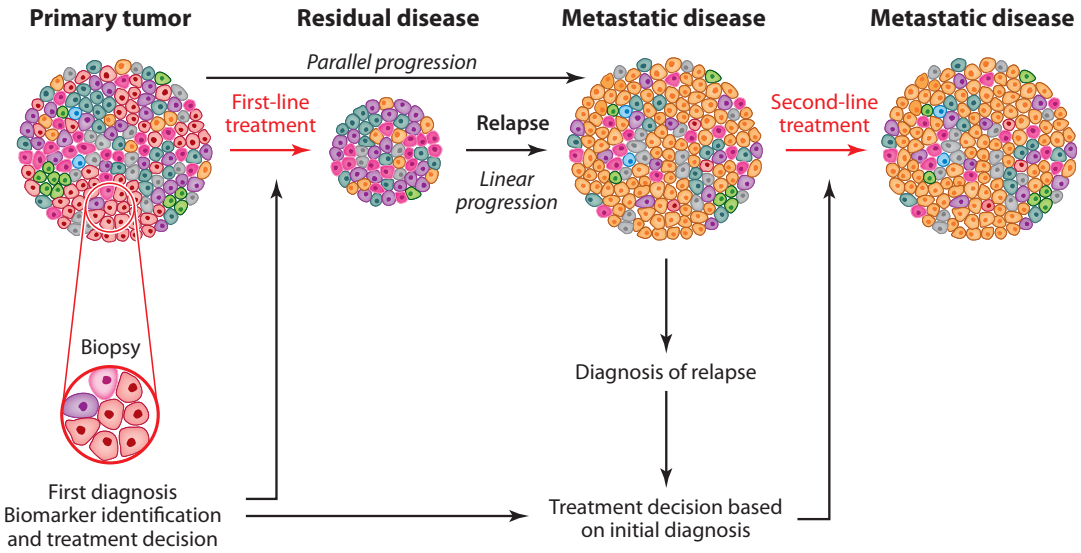

Figure 10 Illustrating intratumor heterogeneity. Typically, cancer diagnosis is based on sampling a subsample of tumor cells (left hand side of the figure) baed on biopsy. Because of inherent heterogeneity there are subsample-to- subsample variations, shown by different colors on the top left. Treatments based on such biopsies are only successful in combating the cells in the subsample. Because of stochastic heterogeneity other clones (shown in yellow) resist the therapy, leading to progression of the disease. Metastases could develop from clones that survived the initial therapy. Consequently, treatments based on initial diagnosis are not efficacious in fighting proliferation at subsequent times, which is an inherent feature of heterogeneity much like in glasses.

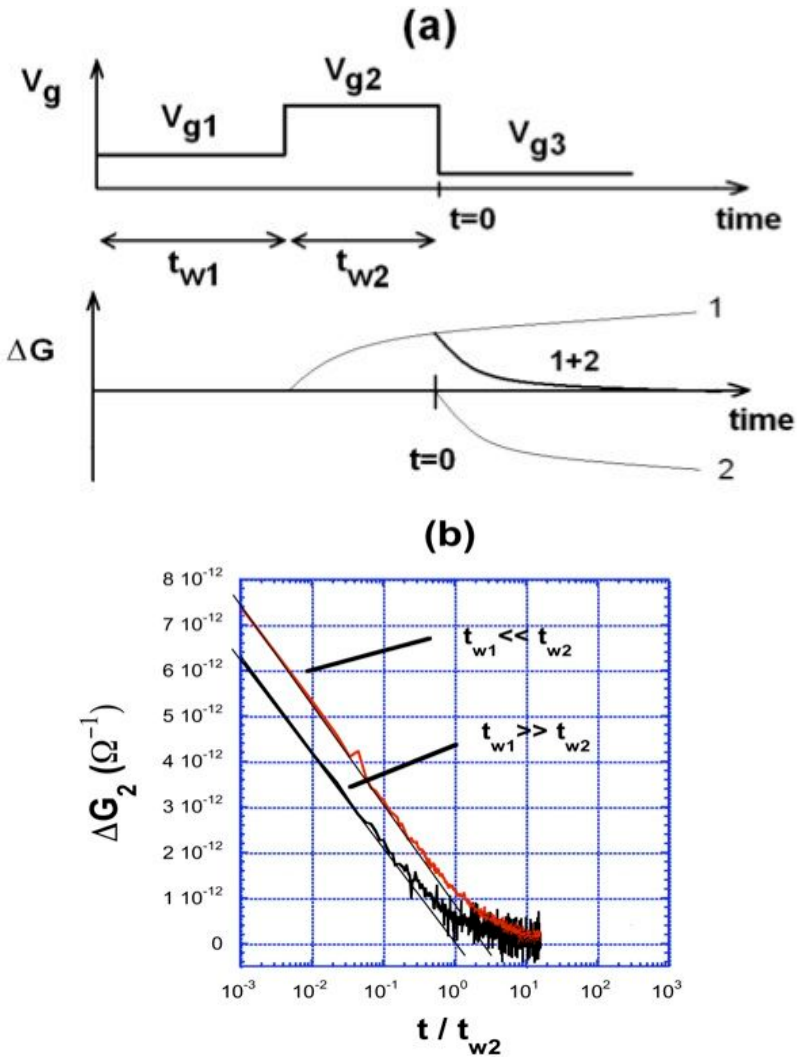

Figure 11 (a) Experimental protocol as described in text. (b) Gate voltage dip as a function of time $t > 0$ for $t_{w_1} \ll t_{w_2}$ and $t_{w_1} \gg t_{w_2}$.

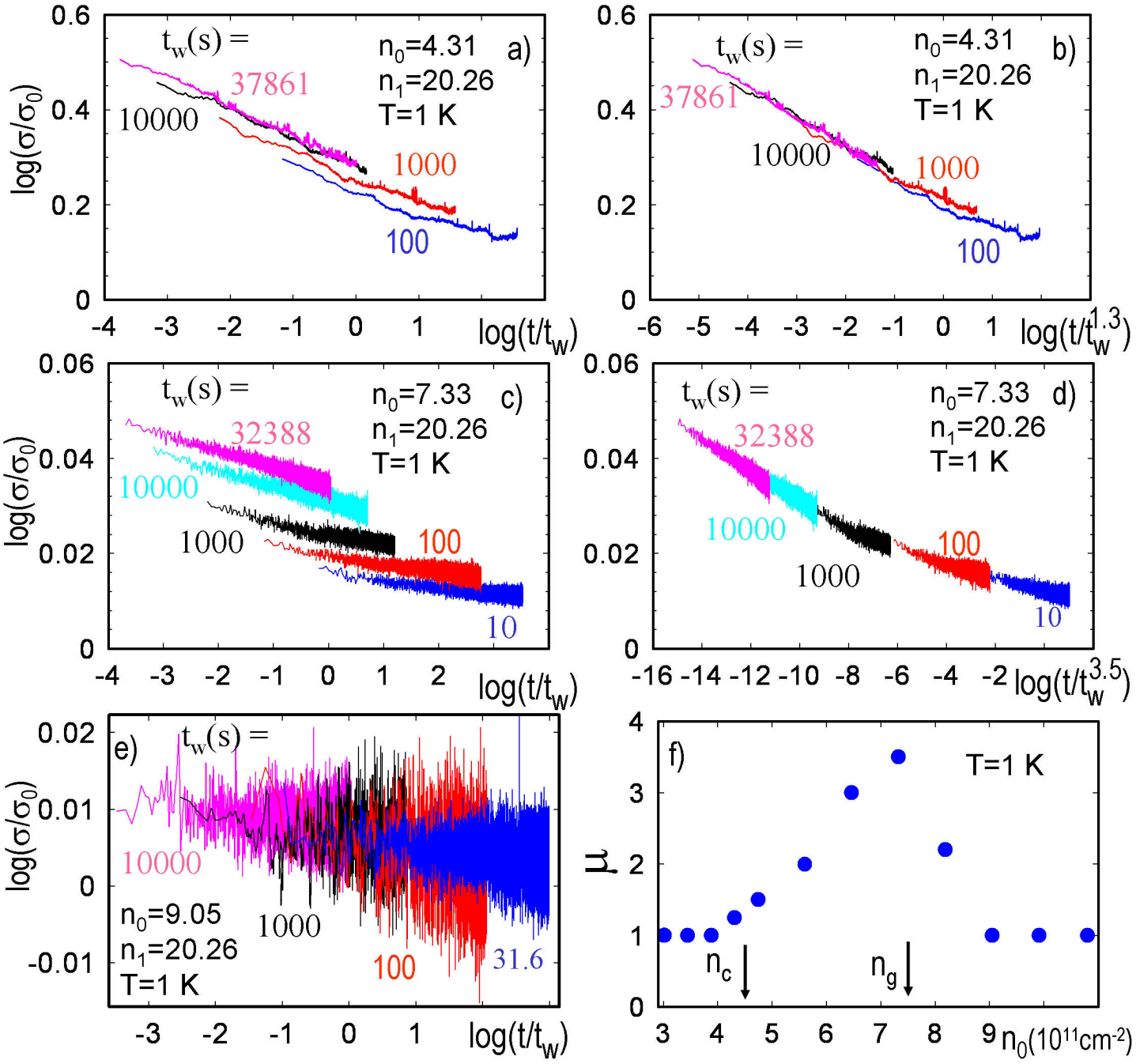

Figure 12 2D MOSFET with initial gate voltage V_0(density n_0) that is changed to a voltage V_1(density n_1) for a time t_w and then changed back to voltage V_0 at a time $t = 0$. $\sigma(t > 0, t_w)$ is measured. (a), (c), (e) Relaxations for different n_0 at fixed n_1, scaled with time t_w. (b), (d) Scaling with t_w^{μ} improves the collaspe of the data. (f) μ vrs n_0 does not depend on n_1.

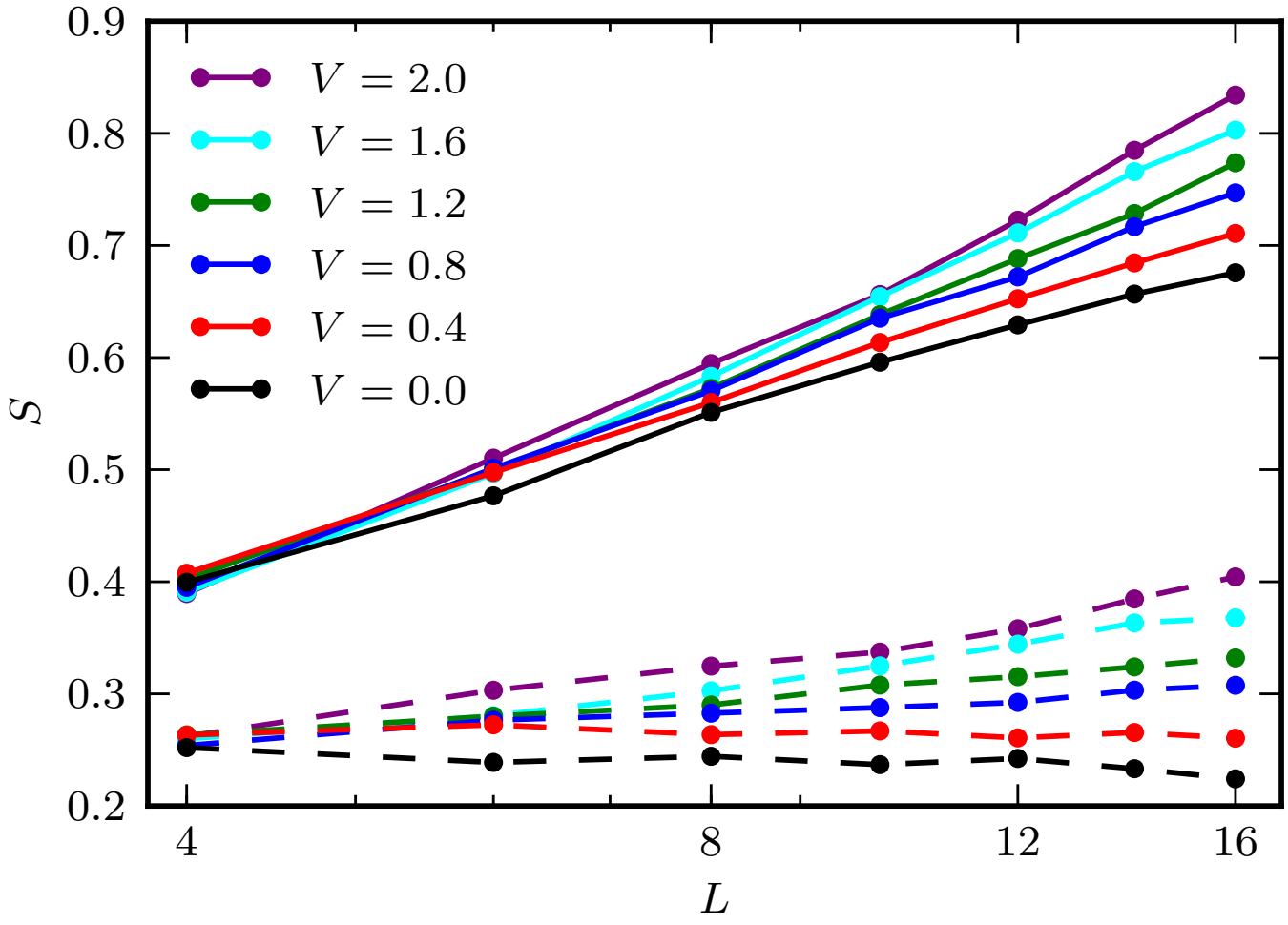

Figure 13 The coefficient $a(L)$ is a measure of the entropy. Solid lines are $W = 8$, dashed lines are $W = 6$; interaction strength is $V = 0, 0.4, 0.8, 1.2, 1.6, 2.0$. In a many body localized regime $a(L \to \infty)$ approaches a constant, while in a metallic state $a(L \to \infty)$ grows linearly with system size.